

Multilayering of Surfactant Systems at the Air–Dilute Aqueous Solution Interface

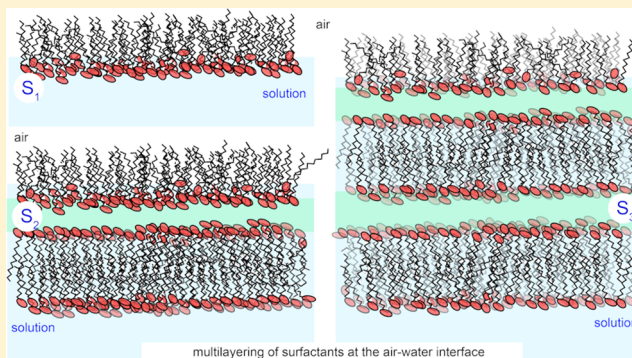
Robert K. Thomas*,† and Jeffrey Penfold†,‡

†Physical and Theoretical Chemistry Laboratory, University of Oxford, South Parks Road, Oxford, OX1 3QZ, United Kingdom

‡STFC, Rutherford-Appleton Laboratory, Chilton, Didcot, Oxfordshire OX11 0RA, United Kingdom

S Supporting Information

ABSTRACT: In the last 15 years there have been a number of observations of surfactants adsorbed at the air–water interface with structures more complicated than the expected single monolayer. These observations, mostly made by neutron or X-ray reflectivity, show structures varying from the usual monolayer to monolayer plus one or two additional bilayers to multilayer adsorption at the surface. These observations have been assembled in this article with a view to finding some common features between the very different systems and to relating them to aspects of the bulk solution phase behavior. It is argued that multilayering is primarily associated with wetting or prewetting of the air–water interface by phases in the bulk system, whose structures depend on an overall attractive force between the constituent units. Two such phases, whose formation is assumed to be partially driven by strong specific ion binding, are a concentrated lamellar phase that forms at low concentrations and a swollen lamellar phase that is not space-filling. Multilayering phenomena at the air–water interface then offer a delicate and easy means of studying the finer details of the incompletely understood attraction that leads to these two phases, as well as an interesting new means of self-assembling surface structures. In addition, multilayering is often associated with unusual wetting characteristics. Examples of systems discussed, and in some cases their bulk phase behavior, include surfactants with multivalent metal counterions, surfactants with oligomers and polymers, surfactant with hydrophobin, dichain surfactants, lung surfactant, and the unusual system of ethanolamine and stearic acid. Two situations where the air–water surface is deliberately held out of equilibrium are also assessed for features in common with the steady-state/equilibrium observations.



INTRODUCTION

Accumulation of surfactant bilayers in addition to the normal monolayer present at an air–water (A–W) interface, i.e. multilayering, has only relatively recently been observed. There are three main reasons for interest in such multilayering phenomena: (i) the A–W interface occurs in a variety of situations, foams, mineral flotation, the lung, and the preparation of some materials, (ii) multilayering seems to be associated with enhanced wetting characteristics, which is a key component of many applications, (iii) systems where multilayering has been observed mostly have bulk phase diagrams in which lamellar phases are formed at dilute bulk surfactant concentrations and the effects of the perturbation introduced by the surface are potentially useful in understanding why these phases form. The advantage of the A–W interface is that it can be characterized thermodynamically and dynamically and therefore links between the bulk surface properties and those on the molecular level, such as layer structure, can be used to establish fundamental understanding.

Figure 1 shows schematically the simplest multilayer systems at the A–W interface, which we designate S_1 , S_2 , and S_3 where the subscript indicates the number of layers. A layer is not

defined here as a molecular layer but as a mono- or bilayer separated by solution from the next layer. S_1 here illustrates the normal adsorbed monolayer at the A–W interface, but at a hydrophilic solid–water interface, it would be some sort of bilayer totally immersed in water. All three surface structures $S_{1–3}$ have been observed. Multilayering with n bilayers is denoted by S_n . However, experiment often does not give accurate values of the number of constituent bilayers beyond three, and there may also be polydispersity across the surface. We use the terms S_M when there are more layers than can be measured at the instrumental resolution and S_m when m can be determined.

Multilayering at the A–W interface of surfactant solutions can be thought of in terms of wetting and prewetting. In a region of two liquid phases, α and β , the A–W interface will consist of whichever phase has the lower interfacial tension with air. If α is more surface-active and is also the less dense phase, it will obviously form the A–W interface. However, it will also

Received: December 21, 2014

Revised: February 10, 2015

Published: February 14, 2015

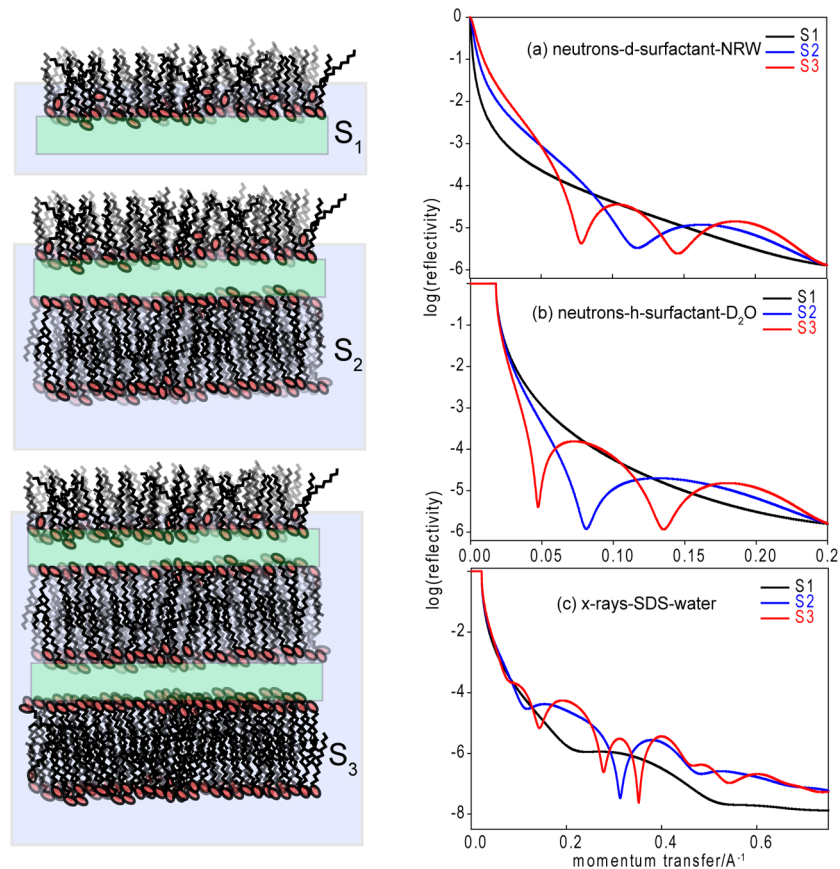


Figure 1. (Left) Schematic drawing of simple multilayer structures that have been observed at the air–water interface with their nomenclature. The blue shading indicates the approximate extent of the immersion of the layer in water, and the green indicates the involvement of an agent other than the surfactant. (Right) (a) and (b) NR profiles calculated for simple model fits for S₁, S₂, and S₃ structures in isotopic compositions of (a) a perdeuterated surfactant in NRW and (b) a normal protonated surfactant in D₂O and (c) the corresponding XRR profiles. The model for NR consists of slab distributions of a monolayer of volume fraction 0.5 and thickness 20 Å and bilayers of volume fraction 0.6 and thickness 25 Å with pure water gaps of 5 Å. A realistic background has been added, and the profiles are displaced vertically for clarity. The model used for the XRR calculation is the same with the contribution of the counterions and headgroup (taken to be that of SDS) added to the aqueous layers.

form a thin film at the A–W interface, i.e., wet the surface, if it is the more dense phase because it lowers the surface free energy. The gravitational effects opposing this are negligible under normal circumstances. Thus, the gravitational energy per unit area lost in creating a layer of thickness t at a height h above the level of the lower phase is $thg\Delta\rho$, where $\Delta\rho$ is the density difference and g is the gravitational acceleration. For a layer of thickness 100 Å at a height of 1 cm and a 10% change in density, this is equivalent to extra energy of 10⁻⁴ mN m⁻¹, which is negligible compared to surface energies. Prewetting can occur when a system is close enough to phase separation that an interface can induce the formation of a thin film of a new phase before it appears as a bulk phase, the familiar example being capillary condensation of a vapor below its saturated vapor pressure into liquid in small pores. Thus, in the previous example, if the point at which phase α separates has not yet been reached, then the extra stabilization provided by its lower A–W interfacial free energy may induce the formation of a thin film at the A–W interface. (See Supporting Information for further references in this area.)

Discussions of wetting and prewetting in the literature are concerned with simple liquids, but surfactant solutions introduce additional complications. Thus, when a lamellar phase forms a prewetting or wetting film, the question arises as to how many layers are needed in the surface film, and this will

depend on the basic features of the formation of lamellar phases. For lamellae to be stable relative to micelles and rods, the packing parameter v/al , where v is the volume, l is the maximum length of the hydrophobic unit, and a is the cross-sectional area in the aggregate, must be between $1/2$ and 1. When this condition is satisfied, a lamellar phase should form as a space-filling structure. The lamellar phase of a surfactant (L_a), which forms at high concentrations of surfactant, is the usual result and is reached because electrostatic screening gradually reduces a as the concentration increases. However, by various devices, e.g., using double-chained surfactants, the packing condition can also be satisfied at low concentrations. In such systems, free lamellae are formed and can remain as such or form a variety of vesicle structures depending on the balance of energies associated with elasticity, compressibility, and edge energy of the lamellae. These are space-filling structures held apart by repulsive forces from diffuse ion distributions and Helfrich undulations.

The addition of a divalent ion, e.g., Ca²⁺, to an anionic surfactant increases the packing parameter of anionic surfactants by binding more tightly to the headgroup and reducing a . This often preferentially stabilizes the solid surfactant phase, which then precipitates and is the cause of the problem of the use of surfactants and soap in hard water. However, an early observation on calcium dodecyloxy sulfonate

(CaC_{12}ES) showed that, rather than precipitation, the addition of divalent ions sometimes causes the separation of a concentrated L_α similar in water content to the normal L_α ¹ phase, i.e., with a repeat spacing in the range of 30–60 Å.¹ Khan et al. found that in other systems a swollen L_α phase is formed, e.g., in sodium di(2-ethylhexyl) sulfosuccinate (NaAOT) and in $\text{Ca}(\text{AOT})_2$.² Khan et al. further showed that CaC_{12}ES not only formed concentrated L_α but could be induced to form swollen L_α by the addition of decanol.³ The important feature of these two new L_α phases is that they can exist only if there are attractive forces between the lamellae, and attractive forces are not part of simple models of colloidal stability. If a surface is attractive to lamellae, then it should be wetted or prewetted by systems that have a tendency to form either of these L_α phases. There is no nomenclature that distinguishes the four L_α phases above, and here we distinguish them with the terms $L_\alpha(n)$ for the normal concentrated lamellar phase, $L_\alpha(sf)$ for the space-filling phase (subdivisions of this phase are not important in the discussion), $L_\alpha(c)$ for the concentrated phase that is formed in dilute solution, and $L_\alpha(sw)$ for the swollen phase.

The factors driving the formation of $L_\alpha(c)$ and $L_\alpha(sw)$ were originally interpreted for divalent counterions by Wennerstrom et al.⁴ Between ionic lamellae there is an exponential repulsive force from the distribution of the counterions in the interlayer, which is expected to dominate the phase structure. Wennerstrom et al. and Guldbrand et al. have shown that the presence of divalent counterions leads to an additional attractive force resulting from ion correlation effects associated with the difference in dielectric constant of hydrocarbon and water.^{4,5} This can drive the system in the direction of $L_\alpha(c)$ at low concentrations of surfactant. The maintenance of the liquid-crystalline form also requires effects that disrupt any crystalline coherence, e.g., a double bond in the hydrocarbon chain, shorter or double alkyl chains, more delocalization of the electric charge, or the introduction of ethoxy groups. Such effects may also cause the system to change from $L_\alpha(c)$ to $L_\alpha(sw)$. At longer distances, the Helfrich undulation force may further assist the formation of the swollen phase. However, it is the attractive force that prevents expansion to $L_\alpha(sf)$ that is more elusive. More recent Monte Carlo simulations have confirmed the earlier conclusions of Wennerstrom et al. that just electrostatic interactions can give rise to both phases.⁶ Experimentally, these effects have been explored in detail for divalent Ca^{2+} by Zapf et al.⁷ and for dialkyldimethylammonium halides by Zemb et al.^{8–10} and Ninham et al.¹¹

The adsorption of an S_1 layer reduces the ST sufficiently that one would expect little extra effect from the addition of more bilayers. Estimates of the surface tension of a free bilayer in water give a value of about 1 mN m⁻¹; therefore, there has to be significant coupling to the monolayer to drive the formation of additional layers.¹² The interaction energy, ΔG_2 , between the initial monolayer and bilayer to form the S_2 structure is likely to be different from the ΔG_3 between S_2 and an additional bilayer to form S_3 . If the lamellar phase has not yet formed as a bulk phase, then this implies that ΔG_3 is small, and if ΔG_2 is large enough, then S_2 will form at the surface but not S_3 or S_m . Closer to phase separation a sufficiently large ΔG_2 will bring about multilayer adsorption, although it will probably be polydisperse in m or M . The pattern of adsorption in these cases will therefore partially depend on the interactions within the bulk phases, but the adsorption of S_m or S_M will approximately correspond to wetting and that of S_2 or S_3 will approximately

correspond to prewetting. Coupling between layers may occur through features of the structure,¹² electrostatic interactions, or bridging. The multivalency of the species that are known to cause the adsorption of S_2 and S_3 structures suggests that bridging by these species may also be important.

There are few techniques that detect multilayer adsorption at the A–W interface. Although the variation of ST with concentration is the standard method for determining the surface excess and the presence of an extra bilayer at an A–W interface leads to a larger surface excess than normal, multilayer formation is usually associated with aggregation in the bulk, and there is then insufficient quantitative information about the bulk activities to apply the Gibbs equation. Nevertheless, ST itself remains an important thermodynamic measurement. Spectroscopic methods, although not generally effective for determining the surface excess in monolayers, can be useful in the multilayer situation as shown by Takumi et al.,¹³ who used the IR intensity to measure extra surfactant above a monolayer. Ellipsometry is sensitive to the surface excess and can detect anomalous excesses above a monolayer,¹⁴ but it cannot resolve multilayer structure. The only generally effective techniques for determining either or both surface excess and structure for multilayers at the A–W interface are neutron reflection (NR) and X-ray reflection (XRR). Thus, the signatures of the S_1 , S_2 , S_3 , and S_M phases may be instantly distinguishable with little further quantitative analysis. The NR profile from a perdeuterated surfactant in null reflecting water (NRW), where there is no signal at all from the water, is particularly effective as shown in Figure 1(a). The slightly easier composition for study is the hydrogenated surfactant in D_2O , shown in Figure 1(b), but it is not sensitive to the outer monolayer. The sensitivity of XRR is more complex. It is very sensitive to the outer part of the S_1 structure because this has a lower scattering length density than the bulk solution. In general, its sensitivity to a layered structure is high if the surfactant is ionic because the greater concentration of electrons in the headgroup region will dominate the scattering. The responses of X-rays to the same structures as in the rest of the figure are shown for the sulfate–sodium combination in Figure 1(c). The packing of the bilayer below the monolayer has been found to be significantly lower than a close-packed bilayer, and this suggests that it may rearrange into some kind of ordered lateral structure. The only technique capable of exploring such structure at the A–W interface is grazing incidence X-ray diffraction (GIXD).¹⁵ Historically, most earlier studies of induced surfactant ordering at interfaces involved a second surface as a probe or part of the confinement, but if a system is going to be affected by a single surface, it will be differently affected by two surfaces and therefore from the point of view of studying just the A–W interface such experiments are to a greater or lesser extent invasive. Nevertheless, such studies are important and are omitted here only for reasons of space. They are well reviewed for polyelectrolyte–surfactant systems by Bergeron and Claesson.¹⁶

It can be difficult to determine experimentally whether equilibrium has been reached at an A–W interface, and often the only guarantee is usually that a steady state has been reached. Possible important factors are that (i) any adsorption or desorption process involving aggregates is always slow, (ii) adsorption on the walls of the container will be different from that at the A–W interface but the two surfaces are in contact and the Marangoni effect ensures rapid transport between them, and (iii) there is continuous evaporation and

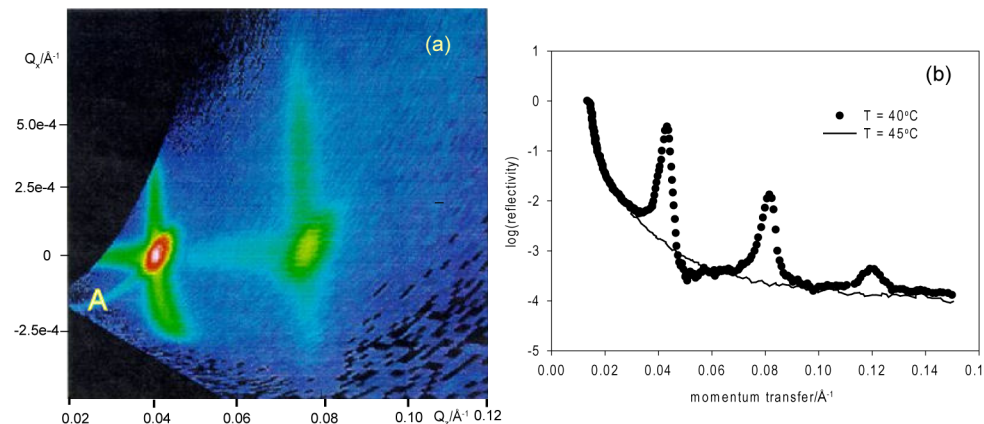


Figure 2. (a) Specular and off-specular neutron scattering from the A–W interface of a 2 wt % solution of AOT in water at 298 K transformed into a map of the scattering in terms of Q_z and Q_x .¹⁷ (b) Specular reflection from the same solution.¹⁸ Note that the change in scattering coordinates is the cause of the unusual shape of the regions where the off-specular signal is nonzero.

condensation of solvent at an A–W interface and this may generate local heterogeneities. The difficulty in either studying these effects or trying to eliminate them is that they are usually all present in systems of interest and the use of dynamic methods to eliminate one or more of them tends to generate new artifacts to replace the steady-state ones. Nearly all of the systems to be discussed below are slow to come to equilibrium, mostly requiring 1–3 h. The NR experiments generally use sealed thermostated containers with large-area samples in Teflon troughs and cycle four to eight samples in a run so that in order to establish whether a steady state has been reached a given sample will usually be in its container for 4 or more hours without disturbance. Factors such as humidity, temperature, and convection are therefore minimized.

In this article, we review observations of multilayering at the A–W interface, using examples from a variety of surfactant solutions with other additives including systems that are deliberately maintained out of equilibrium. For reasons of space, we limit ourselves to the adsorption of layered structures from dilute surfactant systems, which means that we neglect some of the earlier NR and XRR work on the near surface adsorption of micelles and on the surface structure of more concentrated systems.

■ ADSORPTION OF SWOLLEN LAMELLAR PHASES

NaAOT forms an $L_\alpha(\text{sw})$ phase,¹⁹ and the adsorption of this phase has been studied at the A–W, the hydrophilic silica–aqueous, and the sapphire–aqueous interfaces.^{17,18,20,21} At concentrations above about 1 wt %, the bulk solution separates into $L_\alpha(\text{sw})$ and isotropic solution. The bulk lamellar spacing ranges between about 100 and 300 Å and decreases with increasing temperature but is only weakly affected by added NaBr (0.1 and 1 mM). At the A–W interface, a series of sharp Bragg peaks is observed that is characteristic of an S_m structure with a slightly smaller but similarly temperature-dependent repeat spacing (shown for a 2 wt % solution at 25 °C and a d spacing of 175 Å in Figure 2(b)). That this structure corresponds to the adsorbed bulk lamellar phase is suggested by (i) the similar but not identical d spacing, (ii) the temperature dependence of the adsorption (both phases disappear at the same upper temperature of around 65 °C, but desorption occurs at low temperatures, below about 15 °C), and (iii) the effect of the addition of small amounts of electrolyte, which strongly decreases the adsorption but does

not destroy the bulk lamellar phase. That neither gravity nor the humidity gradient (as implied by Aberg et al.²²) is involved is shown by the similar results for the hydrophilic solid–aqueous interface in vertical and horizontal positions and the similarity of A–W and solid–aqueous results. The reversible desorption and adsorption with the change in temperature further indicates that these are equilibrium films. The weakness of the adsorption is indicated by the small change in spacing upon adsorption, which is comparable to the effect of small changes in temperature on the bulk phase and by the ease with which the multilayer is desorbed on lowering the temperature or on the addition of 0.1 mM NaBr. Quantitative modeling of the specular reflection data indicates that the overall thickness of the multilayer is ~0.5 μm (about 25 bilayers). As suggested in the Introduction, the existence of an $L_\alpha(\text{sw})$ phase requires attractive forces between the bilayers, and if adsorption occurs at all it will be of an S_m or S_M structure. This will depend almost entirely on the energy between the monolayer and first bilayer, i.e., ΔG_2 above. This suggests that the desorption on addition of small amounts of NaBr is caused by small changes in the electrostatics close to the surface, which is consistent with a systematic study of undulations in the $L_\alpha(\text{sf})$ of a different system at the solid–liquid interface, which showed that the amplitude of the undulations is substantially less than the d spacing for ionic systems.²³

The off-specular scattering from the AOT multilayer is strong as shown in Figure 2(a), in which the pattern on the original detector has been rescaled so that the data is plotted in terms of scattering vectors Q_z and Q_x normal and parallel to the surface, respectively. The strong ridge of scattering at $Q_x = 0$ is the specular reflectivity shown in Figure 2(b). The remaining off-specular scattering is the response of the scattering to the lateral structure or roughness of the various interfaces. The first models of off-specular scattering were derived by Wainfan et al.²⁴ and Pynn.²⁵ (Further references to off-specular scattering are given in the Supporting Information.) Pynn has shown that strong scattering along Q_x at a fixed value of Q_z corresponding to a Bragg peak is characteristic of a strong but significantly conformal roughness of a multilayer system. Rough layers generate two further off-specular scattering components. These result from the interference of the beam scattered at an upper rough surface with that reflected from a lower smooth surface (Newton's fringes) and vice versa. They depend on the separate incoming and outgoing wave vectors. Such a feature is marked

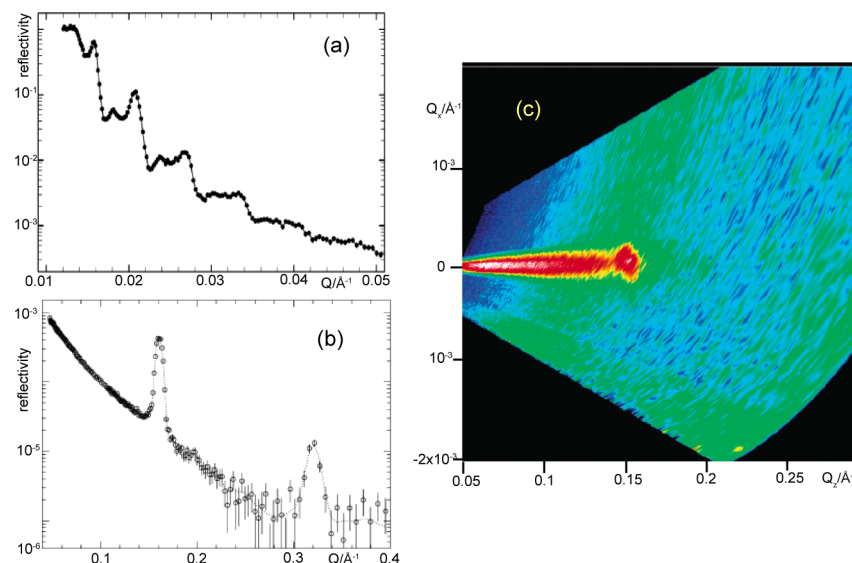


Figure 3. (a) Specular neutron reflection from 2 wt % DDAB in D_2O scattered from the silica–air interface at 65 °C showing the alternation of fringes and peaks. (The profile of this system at 25° is similar, but the alternation effect is less clearly resolved.) The spacing is also different at the two temperatures. (b) Specular reflectivity for 3×10^{-4} M deuterated DHDAB in 0.1 M KBr in NRW at 40 °C with a fitted multilayer model. (c) Specular and off-specular scattering intensity in the Q_z – Q_x plane for the same sample as in (b).^{27,29}

A in Figure 2(a), and this type of feature has also been observed in other unrelated multilayer systems.²⁶ For a single layer, there are interference fringes along the streak,^{24,25} but here the multilayer structure leads to a unresolved streak of intensity which increases strongly at longer wavelengths as the Yoneda scattering is approached. Subsequent experiments on the adsorption of AOT at the sapphire–aqueous interface using grazing incidence small-angle neutron scattering (GISANS), which measures the off-specular scattering directly, showed much weaker off-specular scattering.²¹ However, the pattern of off-specular scattering observed by Li et al. is similar for both A–W and solid–aqueous interfaces and changes in a systematic way compared to that of other surfactants below.

McGillivray et al. have done NR experiments on solutions of didodecyldimethylammonium bromide (DDAB) and diundecyl DAB, DUAB, adsorbed at the A–W interface from 25–45 °C and the silica–aqueous interface from 25–65 °C.²⁷ The dilute solutions are in equilibrium with a monolayer and bilayer of surfactant, respectively, on each of the two surfaces, but in the concentration range of 0.2–2 wt %, similar multilayered structures are formed at both interfaces. Like AOT, the interlayer spacing decreases with increasing temperature and adsorption is reversible with respect to temperature, but unlike AOT, the number of bilayers present at both surfaces is an average of just two, i.e., an S_3 structure. Figure 3(a) shows the unusual NR profile where Bragg peaks alternate with weaker interference peaks. This has only one possible interpretation, which is that the repeat spacing between bilayers is half the total spacing of the layer. Quantitative analysis suggests that there may be some polydispersity across the surface, in which case the maximum number of layers may rise to about four and be patchy. The spacing is also much larger than for AOT, 1600 Å at 25° and 700 Å at 65° for the silica–aqueous interface. The adsorption of such a small number of layers, effectively an S_3 surface structure of large dimension, is consistent with the adsorption of an $L_\alpha(\text{sf})$ phase, unlike the multilayer adsorption from the $L_\alpha(\text{sw})$ of AOT above. Haas et al. observed a mix of different vesicle types in the bulk solution, which could be

$L_\alpha(\text{sf})$, but their lowest concentration at 4% was higher than those of McGillivray et al. and they did not measure the dimensions directly.²⁸ McGillivray et al. used SAXS to estimate the interlamellar spacings, but there was no detailed modeling of the structure. Off-specular reflection was observed along a constant Q_z at the Bragg angle, i.e., the two layers are rough but also significantly conformal. However, the roughness was much weaker at the A–W interface than at the aqueous–silica interface or for AOT at the A–W interface. The coincidence of the almost identical and unusual structures at the solid–liquid and A–W interfaces again verifies that inhomogeneities caused by incomplete equilibration with water vapor are not significant under the typical conditions of the NR experiment.

Penfold et al. have studied the adsorption of the closely related surfactant dihexadecyltrimethylammonium bromide (DHDAB) from dilute solution at the A–W interface²⁹ (although the adsorption is not of $L_\alpha(\text{sw})$; we include it here because of its close relation to the previous example). At a concentration of 3×10^{-4} M, which is above the CMC, DHDAB adsorbs slowly over 3 h as a monolayer over the temperature range of 25–50°. The addition of 0.1 M KBr has, however, a dramatic effect on the surface structure. Below 32 °C, there are only minor changes in coverage. At 32 °C, a sharp Bragg peak appears, corresponding to $L_\beta(\text{c})$ with a repeat spacing of 33 Å. At this temperature, the chains are not molten (signified by the β). At the melting temperature of 40 °C,^{11,30} $L_\alpha(\text{c})$ starts to form with a repeat spacing of 39 Å, and with time, a second-order Bragg peak appears (Figure 3(b)) and $L_\beta(\text{c})$ disappears. The surface structure at this point is an S_M structure with a thickness estimated to be about 1500 Å. That chain melting is responsible for the change in spacing was confirmed by the addition of benzyl alcohol, which is known to lower the melting temperature. As expected, this maintained the $L_\alpha(\text{c})$ spacing down to 30 °C. Finally, the higher degree of surface ordering relative to both AOT and DDAB is illustrated by the smoothness of the surface as shown by the comparison of Figure 3(c) for DHDAB with Figure 2(a).

Although the structure of the bulk solution of DHDAB has been studied by several groups,^{8–10,28} these studies are mainly at higher concentrations than used in the adsorption experiments. Tucker et al. extended the determination of the pure structure down to 1.5 mM and established that it is predominantly approximately space-filling bilamellar vesicles, i.e., $L_\alpha(\text{sf})$.³¹ If this structure were to be maintained in the presence of 0.1 M KBr, then the adsorption would represent a substantial transformation from $L_\alpha(\text{sf})$ to $L_\alpha(\text{c})$. However, the effect of added KBr is known to be quite complex in this system,³⁰ and the discussion of layer interaction energies on adsorption suggests that $L_\alpha(\text{c})$ has already formed in the bulk solution and is attaching weakly to the surface. However, no precipitation was observed during the processes described above.

As a last example, we examine aqueous solutions of the ethanolamine salt of hydroxy-stearic acid, where the interface promotes the formation of a lamellar phase from a different structure.³² The equilibrium solution contains tubes with an internal lamellar separation that varies in the range of 200–450 Å at temperatures from 20 up to 70 °C when the tubes disperse and form micelles. The external diameter increases from about 0.5 μm at 20° to a maximum of 5 μm at 50 °C before decreasing again. The system has a low surface tension, suggesting that the tubes are highly surface-active. Fameau et al. have used NR to show that at 25 °C these tubes adsorb strongly at the A–W interface and are aligned with their long axes parallel to the surface below a monolayer of the surfactant. Given the large interlamellar spacing, which must be associated with relatively weak forces, it is at first sight surprising that the surface does not induce an unravelling of the tubes into a lamellar structure. However, although this does not occur at room temperature, a slow transition into the unravelled state occurs over a very narrow range of temperature of around 50 °C, giving flat bilayers aligned with the surface with a similar spacing to that in the tubes. Consistent with this being driven by the presence of the surface, this is the temperature at which the elastic properties of the bilayer are at their softest, as determined from independent measurements of the Caille parameter.

■ ADSORPTION OF CONCENTRATED LAMELLAR PHASES

Surfactants and Surfactant Mixtures with Metal Cations. The system that exhibits the widest range of surface multilayers so far observed is that of the metal alkyl ethoxy sulfates, e.g., $\text{C}_n\text{H}_{2n+1}(\text{OC}_2\text{H}_4)_m\text{SO}_4\text{M}$, designated here as $\text{MC}_n\text{E}_m\text{S}$. (We use the common abbreviation SLES for $\text{NaC}_{12}\text{E}_1\text{S}$.) As already discussed, these surfactants have long been known to be extremely effective at resisting precipitation by Ca^{2+} ions. Although Ca^{2+} causes features that might lead one to expect multilayer formation at the surface, no multilayer formation has so far been observed for $\text{Ca}/\text{NaC}_n\text{E}_m\text{S}$ on their own. However, experiments by Alargova et al. using ST and light scattering show that the addition of the Al^{3+} ion leads to several of the features that might be associated with the adsorption of multilayers, e.g., a rapid increase in micellar size above a low CMC.^{35,36} Using this work as a basis, Petkov et al. used NR to observe a sequence of layer structures at the A–W interface of mixtures of SLES and nonionic cosurfactant $\text{C}_{12}\text{E}_{12}$ upon addition of $\text{NaCl}/\text{AlCl}_3$ mixtures.³⁷ Penfold et al. had earlier found that the addition of CaCl_2 induced the formation of S_2 and S_M structures in sodium 6-dodecyl benzene/ C_{12}E_8

mixtures.³⁸ Both of these use the addition of a nonionic surfactant to stabilize potential $L_\alpha(\text{c})$ formation. Subsequently, Xu et al. used NR to make an extended study of the effects of alkyl chain length, ethoxy chain length, and different trivalent metal ions on the surface structure of a series of pure $\text{NaC}_n\text{E}_m\text{S}$ without any surfactant additives.^{33,34,39,40} Although these were not the first experiments to observe extensive surface multilayering, they provide an excellent basis for discussing the phenomenon as a whole.

The addition of different fixed concentrations of AlCl_3 to SLES at low levels causes a strong decrease in the surface tension (Figure 4(a)) at concentrations well below the CMC of

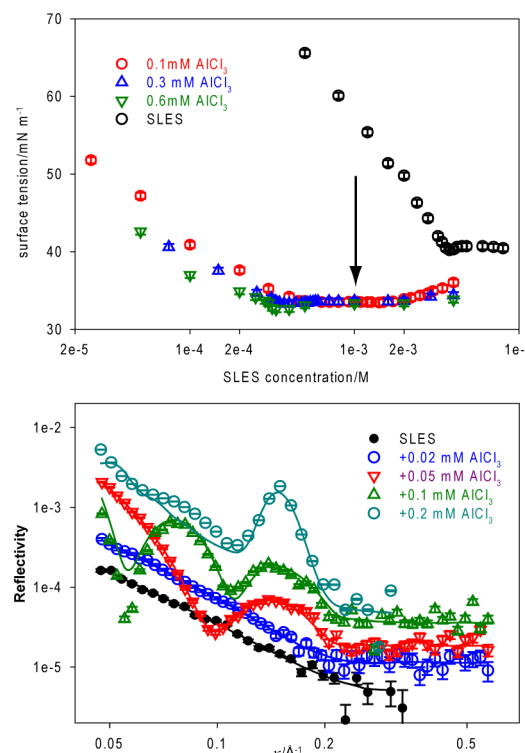


Figure 4. Effects of the addition of different concentrations of AlCl_3 on the surface tension of SLES ($\text{C}_{12}\text{H}_{25}(\text{OC}_2\text{H}_4)\text{SO}_4\text{Na}$) and on the neutron reflectivity (NR) of 1 mM SLES. The NR profiles evolve from a monolayer (S_1) through surface structures S_2 and S_3 to multilayer structure S_m . The arrow marks the concentration of the NR measurements.^{33,34}

SLES, and the tension does not rise to the limiting value for SLES on its own until well above its usual CMC. NR experiments on the surface at the fixed concentration of SLES marked with an arrow in Figure 4(a) show an increase in the adsorbed amount with added AlCl_3 and the evolution from S_1 through S_2 and S_3 to multilayers S_M or S_m shown in Figure 4(b) with the characteristic fringe structures already shown in Figure 1. Features of note are (i) that the solutions are completely transparent except for the highest AlCl_3 concentration, when the solution becomes turbid, (ii) the equilibration time for the formation of the surface layer is typically about 1 h, and (iii) the NR measurements were made on chain-deuterated SLES in NRW, which means that the surfactant is significantly more dense than the solution. The Bragg peaks from the multilayer vary in width, indicating the formation of both S_m and S_M layers. The complete set of measurements leads to surface phase diagrams of which the two pairs in Figure 5 show how

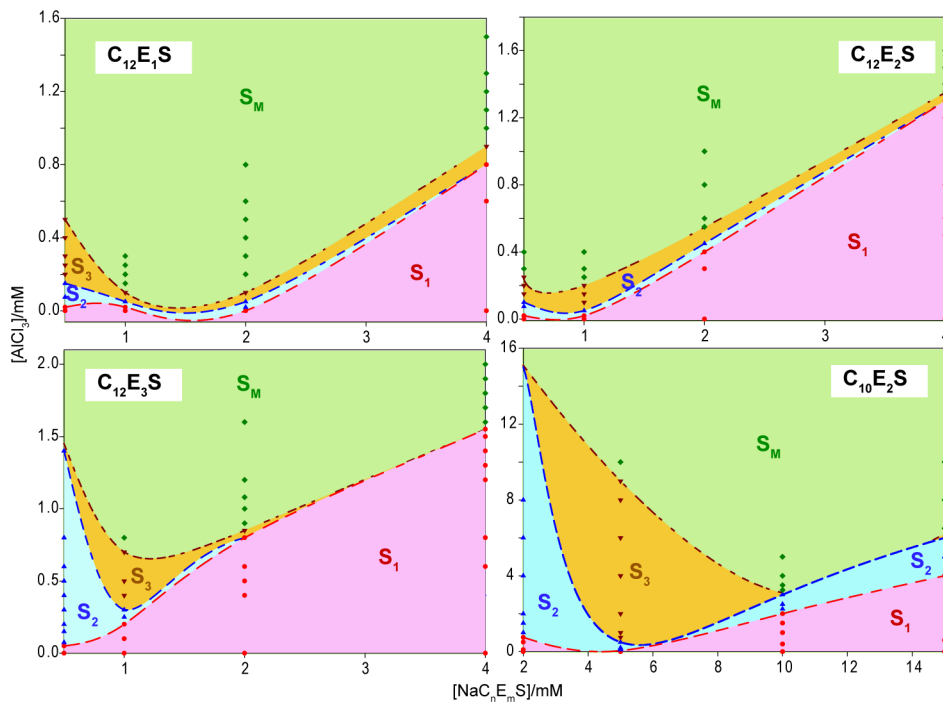


Figure 5. Surface phase diagrams illustrating how an increase in headgroup size ($C_{12}E_mS$) and a decrease in the alkyl chain length (C_{12} and C_{10}) favor the S_2 and S_3 surface structures of alkyl ethoxy sulfates. The points marked on the phase diagrams correspond to NR surface measurements.^{33,34}

surface phases S_2 and S_3 are favored by an increase in the size of the ethoxylate group ($C_{12}E_1S$ and $C_{12}E_3S$) and by a decrease in the alkyl chain length ($C_{12}E_2S$ and $C_{10}E_2S$). Comparable phase diagrams were also determined for C_{14} and C_{16} , and these very clearly show the path from the soluble concentrated lamellar phase to insolubility (Figure 6). As the alkyl chain length increases to C_{14} , the extended multilayer structure S_M is reduced to a small and disordered number of layers, i.e., S_M is replaced by S_m , and then when the alkyl chain is extended to C_{16} , this phase becomes an insoluble precipitate. Apart from the direct evidence of a precipitate in this case, the reduction of the surface structure to a monolayer is also a signature of precipitation. When another ethoxylate group is added to the C_{16} compound, it stabilizes the region over which the S_3 structure is stable, but the final phase is still only the monolayer characteristic of the insoluble precipitate.

Although Figure 1 shows schematically how the shape of the NR profile develops with additional bilayers, detailed fitting can reveal more detail. The development of the characteristic NR profile of the S_2 and S_3 phases as a function of the number of ethoxylates is shown in Figure 7(a,c) together with model fits and gives a quantitative measure of how the additional ethoxylates affect the surface structure. The most obvious effect is on the spacing between the initial monolayer and the first bilayer. In the case of the S_2 structure, the thickness of this layer for the C_{12} surfactant is 7, 10, and 12 Å for E_1 , E_2 , and E_3 respectively, and for the S_3 structure, the d spacing is correspondingly 36, 43, and 46 Å. Because of the wider range of stability of S_2 , it was possible to study several different isotopic contrasts, and the fits of a single structural model with only minor variations to a set of nine different isotopic compositions are shown in Figure 7(b). The level of reproducibility for such different density relationships and the transparency of all of the solutions used for this set of measurements are strong indications that these are equilibrium

structures. Although the structures of the bulk phases cannot be determined at the same low concentrations of the surface experiments, the observed equilibrium behavior of strong micellar growth on addition of $AlCl_3$ with an evolution through rods to an $L_a(c)$ phase is qualitatively consistent with the surface observations.³⁹ A final feature of note for the Al^{3+} - NaC_nE_mS systems is that they are unusually powerful wetting agents in the multilayer regime, e.g., they wet Teflon.

Because Al^{3+} as a counterion has such a dramatic effect in promoting the stability of bulk $L_a(c)$ and the stability of S_2 and S_3 surface structures, Xu et al. also studied the effects of four other trivalent ions, Cr^{3+} , Sc^{3+} , Gd^{3+} , and La^{3+} . Al^{3+} is strongly hydrated, and Cr^{3+} is the only one of the other four to be significantly hydrated. All four ions enhance the formation of the monolayer S_1 of $NaC_{12}E_2S$ to much higher M^{3+} concentrations than Al^{3+} , but except for Cr^{3+} at higher concentrations of surfactant (1 mM $NaC_{12}E_2S$), which has an intervening S_2 structure over a significant range of concentration, they then change to multilayer S_M adsorption. Switching to $NaC_{12}E_3S$ to gain the softening effect of an extra ethoxy group causes the S_2 structure to intervene between S_1 and S_M for Gd^{3+} , but now the Cr^{3+} ion causes only monolayer formation over the whole concentration range. The observation that the presence of a monolayer only can also be a sign that precipitation is occurring might suggest the same here, but the Cr^{3+} solutions remain transparent over the whole range. Just as for the E_2 compound, monolayer formation persists to much higher concentrations of M^{3+} compared to concentrations of Al^{3+} . Further references that have studied the interactions of trivalent ions with anionic surfactants in bulk solutions, although not from a structural point of view, are given in the Supporting Information.

Oligoelectrolytes and Surfactants. The charge separation on oligoions is unlikely to match the preferred packing requirements for surfactant crystallization and should therefore

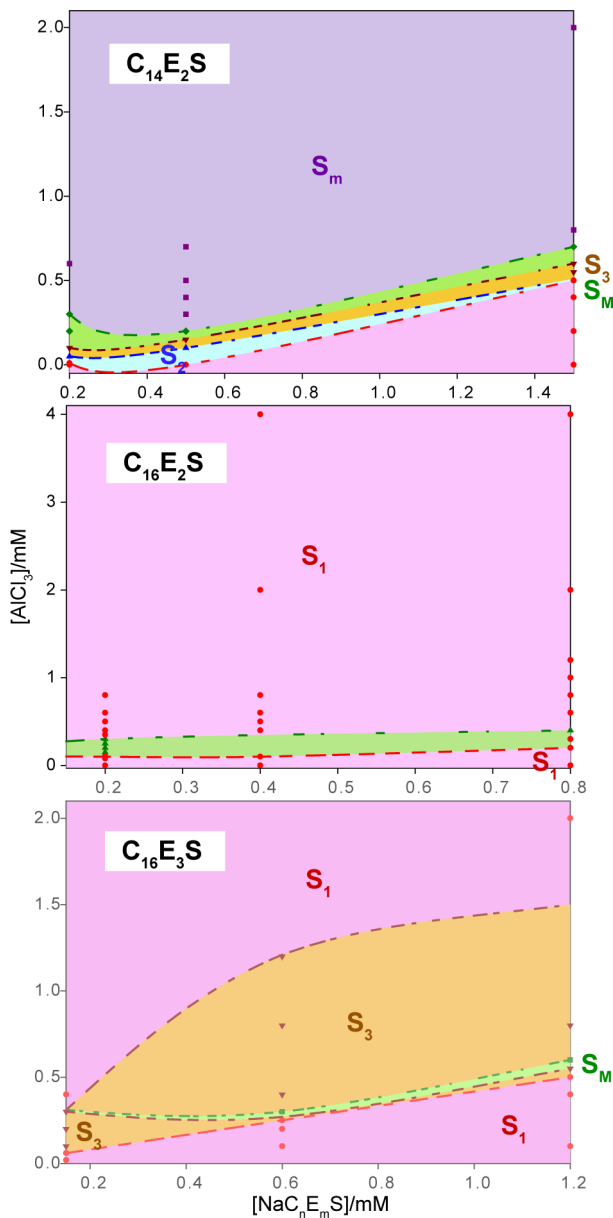


Figure 6. Surface phase diagrams illustrating how a further increase in the alkyl chain length leads eventually to precipitation after a reduction of the thickness of the S_M multilayer. The points marked on the phase diagrams correspond to NR surface measurements.^{33,34}

be better than simple metal ions at stabilizing $L_a(c)$ and hence multilayer surface structures. As they increase in size, oligoions are also likely to have conformations that naturally create bridging links for promoting attraction between the bilayers. It is then not surprising that oligoions form multilayered surface structures with surfactants that otherwise have not yet been observed to form multilayers.

The main series of oligoelectrolytes so far studied are the ethylene imines (EIs), which are the small versions of the polymeric form (PEIs). PEI and polymers based on it are used in a wide range of applications, many of them utilizing their strong interaction with anionic surfactants. The division between oligo and poly is artificial, and here we use oligo to indicate a compound that is not only small but also well-defined in terms of architecture and size. OEs can be controllably prepared in linear or branched form, but PEIs are normally

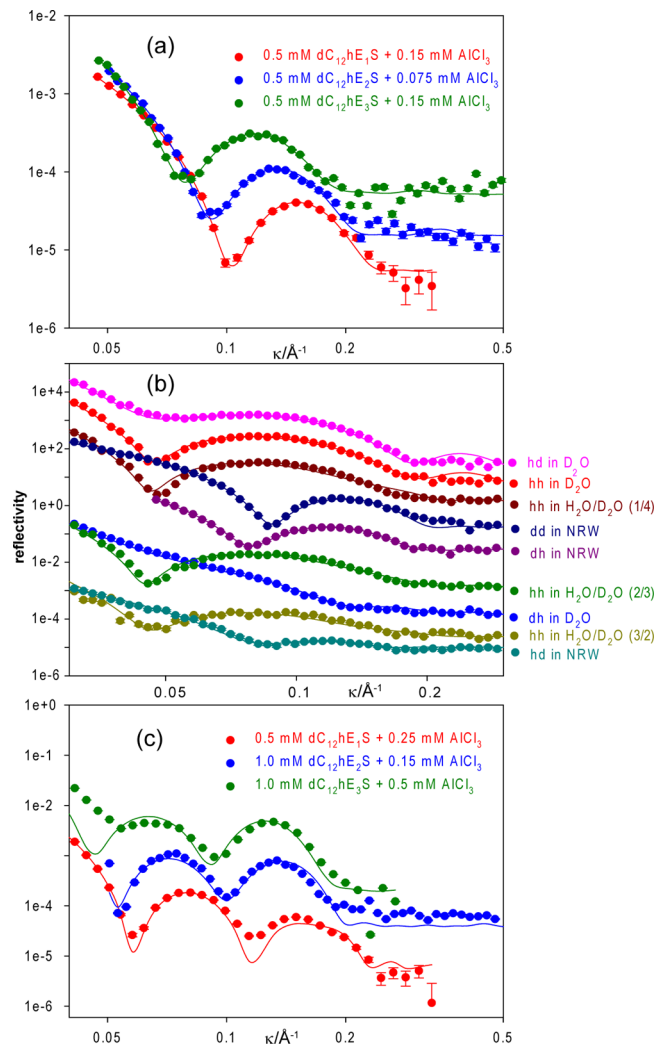


Figure 7. Characteristic NR reflectivity profiles of the S_2 and S_3 surface structures for deuterated $\text{NaC}_{12}\text{E}_m\text{S}$ in NRW and the fits of structural models (a) S_2 and (c) S_3 . Note that the momentum transfer axis is quadratic for these two plots. (b) Fits to nine different isotopic compositions of the S_2 structure for $1.0 \text{ mM } \text{NaC}_{12}\text{E}_3\text{S}$ in the presence of $0.25 \text{ mM } \text{AlCl}_3$.^{33,34}

uncontrollably branched, although they can be prepared in linear form by the hydrolysis of a precursor polymer. The individual primary, secondary, and tertiary amine groups that occur in branched PEIs are weak bases and are extensively protonated at pH 3,⁴¹ weakly protonated at pH 7, and approximately uncharged at pH 10. As well as the charge interaction, these groups are dipolar and can also engage in hydrogen-bonded networks.

Zhang et al.⁴² used NR, with deuterated surfactants in NRW, and ST to study the interaction of a series of commercially available small amines from ethylene diamine to pentaethylene hexamine ($N = 2,3,4,6$ where N is the number of charged groups) with three anionic surfactants—SDS, 6-dodecyl benzenesulfonate (abbreviated here as LAS), and LiDS. At concentrations well below the normal CMC, there is a strong interaction of all of the amine species with the anionic surfactants at pH 3, but this is much weaker at pH 10, as would be expected from the state of ionization. However, with an increasing number of amine groups the difference between the strength of the interaction at pH 3 and 10, as measured by

adsorbed SDS, is substantially reduced, indicating that there is a significant cooperative contribution that offsets the nearly zero charge at pH 10. At pH 10, the smallest three compounds with $N = 2, 3, 4$ do not cause the adsorption of SDS as anything other than a monolayer, but the $N = 4$ and 6 compounds cause the adsorption of thick and well-defined multilayers with first- and second-order Bragg peaks and repeat spacings of 39 ± 0.5 Å. That the interaction is different between pH 10 and 3 is confirmed by the higher repeat spacing at pH 3 of 40.5 Å. At pH 3, the pattern of multilayer adsorption is more erratic, and there is no adsorption of the S_2 structure under any conditions. We note here that, unlike the S_1 , S_2 , and S_3 structures, it is difficult to assess the extent of coverage of a surface by the S_M structure because too many factors contribute, e.g., polydispersity (varying stack size) and structural defects.

Above $N = 3$, the commercial OEIs are not pure isomers and contain some branched material. When aspects of the experiments of Zhang et al. above were repeated with well-defined linear samples, the $N = 3$ and 4 oligomers adsorbed with SDS in the S_2 form at pH 3,⁴³ indicating a weaker tendency to form multilayers, but the $N = 5$ and 6 oligomers adsorbed only monolayers at this pH. The combined results suggest that although the OEIs at pH 3 interact more strongly with monolayer SDS than at pH 10 they interact less strongly with bilayers, and this difference becomes more marked as the OEI length increases. The effect of branching was tested by Halacheva et al. using pure forms of the linear and branched OEI with $N = 8$ and 10, e.g., l-EI₈ and b-EI₈.⁴⁴ Both lead to strong adsorption of monolayer SDS. l-EI₈ shows no multilayer adsorption with SDS at all at pH 3, confirming the conclusion of the previous paragraph. However, it does adsorb as S_M multilayers at pH 7 but less so at pH 10. In contrast, branched b-EI₈ adsorbed strongly as S_M multilayers at pH 3 and pH 7 but not at pH 10. Finally, Halacheva et al. confirmed with ST and NR measurements on l-EI₆, l-EI₁₂, and l-EI₄₀ (MW = 2000) the trend that an increasing chain length of linear OEI at first leads to adsorbed multilayers only at high pH, but then this declines and becomes weak again at MW = 2000.⁴⁵

The strong charge interaction at pH 3 clearly dominates the surface packing of the SDS in a way that makes it unfavorable for there to be any further attachment of a bilayer (or multilayers). One of the advantages of NR when the surfactant is deuterated in NRW is the easy determination of the surface excess, and this gives some clue as to the problem with the packing. The presence of l-EI₈ increases the surface excess of SDS to an average of $4.7 \mu\text{mol m}^{-2}$ at pH 3 (average of nine different [SDS]) but only to $4.1 \mu\text{mol m}^{-2}$ at pH 10 (average of six [SDS]). The presence of b-EI₈ leads to a surface excess of $4.3 \mu\text{mol m}^{-2}$ at pH 3 (two [SDS]) and $3.7 \mu\text{mol m}^{-2}$ (six [SDS]) at pH 10. If the bilayer favors a value of about $4.0 \mu\text{mol m}^{-2}$, then the linear OEI will then favor multilayer structures at pH 10 but not at pH 3 and the branched form will show the opposite trend, as observed. The packing of the surfactant is thus much tighter on the fully charged linear OEI. This could simply block access to a proportion of the charges. However, it could also change the type of aggregate the micelle forms in conjunction with the polymer, by forming cross-links. The interaction with the lowest-charged OEI is reduced for both species but is still strong enough to promote interfacial multilayers for the linear OEI. The details of this interaction are not known, but we note that, in addition to any residual charge interaction, the amino group is strongly dipolar, which could lead to a significant ion–dipole interaction, and hydrogen

bonding is also possible. Either of the last two factors would make it possible for OEI to interact significantly with cationic as well as anionic surfactants, and this will be discussed in connection with PEI in a later section. We emphasize that the formation of multilayers requires the cooperativity of the headgroup interaction and the hydrophobic interaction in the chains. It may be a coincidence that the optimum surface excess for SDS to form multilayers with OEIs is the same as the value for pure SDS at its CMC, and this point will be discussed further below.

One clear result of the above is that the balance of forces required to form the S_2 surface structure is delicate and exists only in a narrow range of conditions whereas S_m or S_M adsorption at an interface can occur over a wider range of conditions. The only observation of the S_2 structure for SDS is with $N = 3$ and 4 linear oligomers at pH 3. With the commercial amines, LiDS and LAS, which have lower Krafft temperatures, i.e., can be thought of as more fluid, were also adsorbed as the S_2 structure, LiDS with the $N = 3$ and 4 oligomers at pH 3 and LAS with the $N = 2$ and 6 isomers at pH 3 (LAS adsorbs as S_M multilayers at pH 10). There are several interesting comparisons to be made between OEI and PEI, and these are made below.

So far, we have not discussed the possibility of phase separation. For the EIs above, precipitation occurs at pH 3 and pH 7 for most of the OEIs studied in a small concentration range centered on the nominal equivalence point. However, at pH 10 the solutions remain clear. Precipitation should not significantly affect the final state of the surface, as already discussed, although it may affect the equilibration time. All of the OEI experiments were done with deuterated surfactant in NRW, ensuring that L_a(c) is the more dense phase. A study of the interaction of the cationic surfactant, C₁₂TAB, with the series of arene sulfonates, POS_n, of which POS₆ is shown in Figure 8, gives a much clearer picture of the phase separation⁴⁶ and its relation to the surface. Four POS_n were studied with $N = 2, 3, 4, 6$. The ST of mixtures of the two smallest with C₁₂TAB behave like single surfactant solutions with a well-defined CMC substantially lower than for pure C₁₂TAB but depending on the POS_n concentration. The solutions also have small-angle neutron scattering patterns characteristic of spherical micelles. POS₄ and POS₆ phase separate, and the separation can be followed by the strong fluorescence of the arene sulfonate, which is bright green in the more dense phase containing the POS_n-C₁₂ complex and blue for the uncomplexed arene sulfonate. The stages of the phase separation are shown schematically for POS₄ in Figure 8, from which it can be seen that the majority of the arene sulfonate is in the lower complex phase. However, measurement of the equilibrated surface with NR, using deuterated C₁₂TAB in NRW, showed enhanced adsorption above a monolayer for POS₄ and the complete formation of the S_2 structure for POS₆, as shown in Figure 8. Although phase separation occurs for POS₄ and POS₆, the shape of the ST curve for POS₄ is little different from those of POS₂ and POS₃, and the only difference in the ST curve for POS₆ is that the main plateau shows a small further drop at high concentrations, which is also a characteristic of polyelectrolyte–surfactant interactions and will be discussed further in the next section. The strong stability of the S_2 structure in the POS₆ system must come about in large part because of the planar structure of the arene sulfonate molecule, which will favor alignment with a surface. However, the surface density of C₁₂TAB may also play

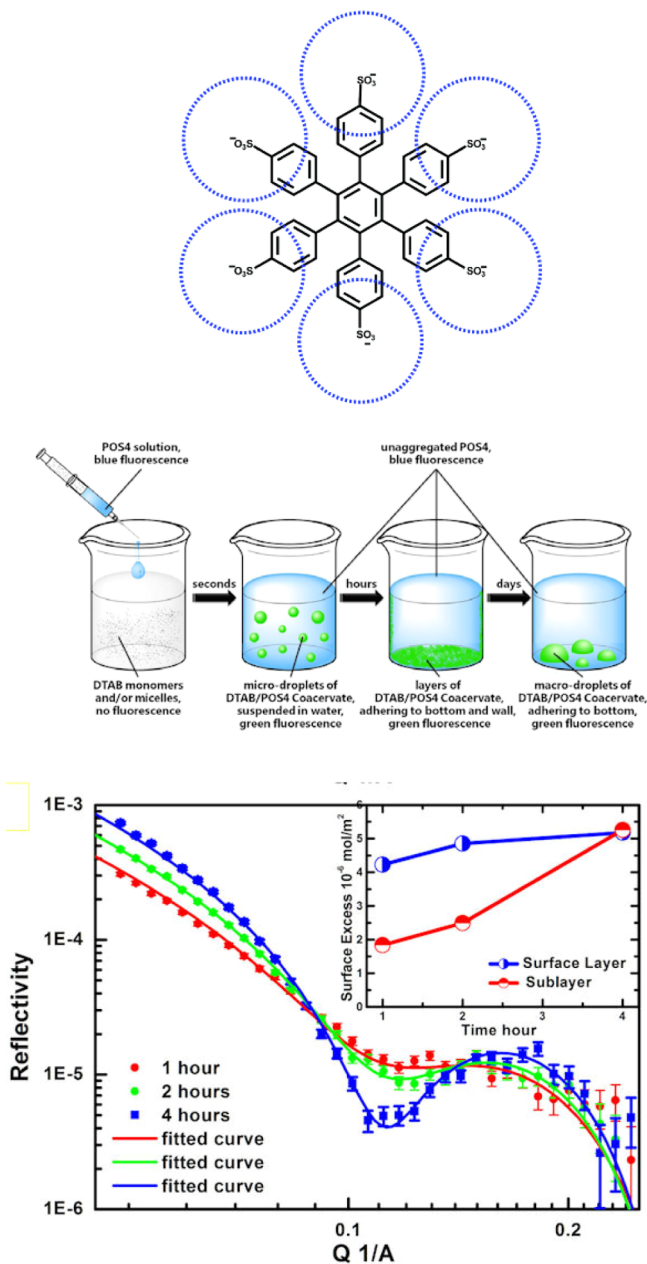


Figure 8. (Upper) Structure of sodium oligoarene sulfonate with six charges (POS_6) with the cross-sectional areas of six vertically oriented C_{12}TAB superimposed as dashed circles above the charged groups. (Middle) Schematic diagram of the phase separation in aqueous mixtures of POS_4 and C_{12}TAB at room temperature. (Lower) Neutron reflectivity profiles of $\text{POS}_6/\text{dC}_{12}\text{TAB}$ in NRW at 1 mM and the development of the surface substructure of C_{12}TAB with time. All data are taken from Jiang et al.⁴⁶

a role as for SDS and the OEI above. It is also close to its pure CMC value at the onset of the ST plateau for the POS_n .

Polyelectrolytes and Surfactants. The promotion of surface multilayer formation of oligoelectrolyte–surfactant mixtures was attributed above mainly to the separation of charges along the chain and their interplay with the requirements of the surfactant. Polyelectrolytes (PE) generally have a more complex charge distribution than either of the OEIs considered above. Thus, the charges on most PEs are pendant and may be some distance from the backbone while the distance along the chain is often just the length of a vinyl

group, in contrast to the OEI or PEI, where the charges are part of the chain. The separation of charges is thus well-defined and unchangeable in the PEI, whereas in the basic helical conformation of a vinyl-based polymer the charge separation depends strongly on the rotational angle. A PE with pendant charges then has a natural possibility of establishing cross-links between layers. As the molecular weight increases from a small value, this should create more opportunities for cross-linking between monolayer and bilayer than in PE of the PEI type, although chain entropic terms may increasingly prevent ordering at higher molecular weight. We discuss complexes of the two types of PE separately.

Until now, a higher fraction of pendant charge PE–surfactant mixtures have been found to exhibit the S_2 structure than any other class of surfactant mixtures. Figure 9(a) shows the

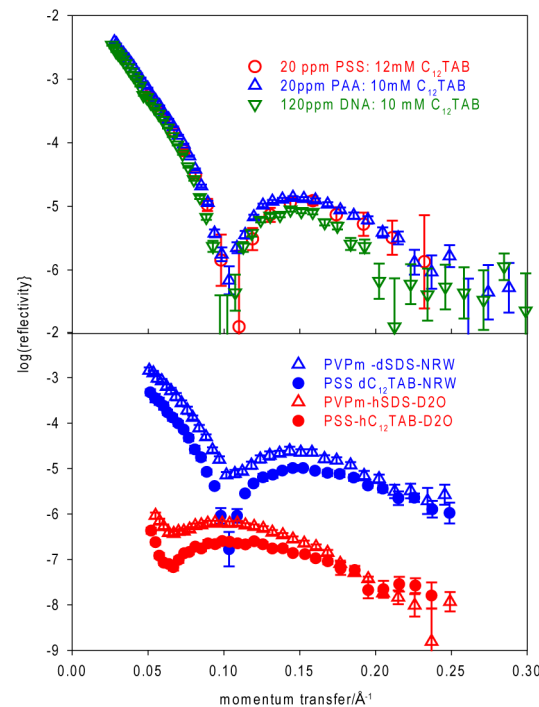


Figure 9. Observed neutron reflectivity for (top) mixtures of 10 mM C_{12}TAB mixtures with three different polyelectrolytes—DNA, PSS, and PAA—in NRW with the surfactant deuterated and (bottom) mixtures of PSS– C_{12}TAB –0.1 M NaBr and PVPm–SDS–0.1 M NaCl, either in NRW with deuterated surfactant or in D_2O with protonated surfactant.^{47–50}

characteristic S_2 signature (Figure 1) in the NR profiles from three mixtures with the same cationic surfactant, C_{12}TAB , but three quite different PEs, DNA, poly(sodium styrenesulfonate) (PSS),^{47–49} and poly(sodium acrylate) (PAA),⁵⁰ and Figure 9(b) compares the results from PSS– C_{12}TAB and poly(vinylpyridinium chloride) (PVPm) with SDS in two different contrasts.⁵¹ The resemblance of the two reflectivity profiles of completely different systems to each other and to the two simple profiles in Figure 1 is striking. The two sets of profiles in Figure 9(b) are in an electrolyte, and PVPm–SDS does not form the S_2 structure in the absence of electrolyte. The PAA– C_{12}TAB system in Figure 9(a) was examined at pH 9 and does not show the structure when the pH is lowered to 3, where the polymer is neutral. The S_2 profile has also been observed for PSS with C_{10}TAB and C_{14}TAB but not C_{16}TAB and also for PEI–SDS. All of the above observations have been made with

NR, but there is confirmation of the presence of a thicker layer than the usual S_1 for PSS–C₁₂TAB behavior from the ellipsometry measurements of Monteux et al.¹⁴ The solution conditions for all of the above observations were a low concentration of PE, usually 100 ppm or less, and a concentration range of surfactant significantly greater than the equivalence point and extending from this point up to about the CMC or even higher. The solutions all phase separate in this region into a concentrated phase, which contains most of the polymer, and a dilute phase in the same way as does the POS_n–C₁₂TAB system. Equilibration of the surface typically takes 1–4 h depending on factors such as the molecular weight. Bragg peaks, i.e., S_M or S_m structures, are only occasionally observed in these systems, indicating that the formation of more extended structures is hindered by an increase in the disorder with the number of layers. When Bragg peaks are observed, they often fluctuate with time and occur over much narrower ranges of concentration than the S_2 structure, i.e., they are not necessarily thermodynamically stable at the surface. Finally, we emphasize that the S_2 structure appears to cover the surface completely. NR is not sensitive to lateral inhomogeneity, but the concentration of surfactant in the bilayer is high and the scope for inhomogeneity is therefore small but would not exclude a regular structural inhomogeneity.

Some PE–surfactant mixtures of the same structural type form no surface structures other than a monolayer, although they also interact strongly and generate monolayer (S_1) coverages and a low ST at concentrations on the order of CMC/100. As the surfactant concentration increases, this group of systems does not maintain the ST at a low value, in contrast to systems that form S_2 layers. There has been much debate over the reasons for the difference, especially over whether both phenomena are dominated by nonequilibrium issues. The discussion is further complicated by the phase separation, although as outlined in the Introduction the surface structure should not be affected strongly by phase separation. It is also complicated by the fact that in a typical ST measurement the composition of the system is being varied with respect to the composition and concentration of the small ions in the system. A recent model of the ST behavior taking these factors into account has been given by Bahramian et al.,⁵² and the nonequilibrium issues have been discussed by several authors.^{53–56} The feature that is different from the systems considered in previous sections is the formation of persistent colloidal aggregates, often dependent on the preparation protocol. The presence of such aggregates would mean that strictly speaking the system is not at true equilibrium, but the effect of this on the surface structure may be small or negligible. This is partially because the surface structure generally varies much less than the bulk (e.g., colloidal aggregates are unlikely to adsorb) and any surface structure is therefore maintained with only minor changes over a wide variation in the equilibrium or nonequilibrium state of the bulk solution. Some support for this comes from Mezei et al., who have shown that in the poly(vinylamine)–SDS system preparation protocols do not affect the surface properties, although they strongly affect those of the bulk solution.⁵⁴ For the purposes of this article, we note that the S_2 layer structure (i) is almost identical in several totally different PE–surfactant systems, (ii) is a coherent structure over the whole surface, (iii) is especially stable in relation to S_m and S_M structures, (iv) is similar to the surfactant layering in the presence of multivalent cations, which are probably at equilibrium, and (v) is remarkably persistent in

time and concentration. All of these factors indicate that at worst it is a stable steady-state structure close to equilibrium *for the surface*, even though it may not be at full equilibrium. However, it is always exceedingly difficult in any surface experiment to prove that surface equilibrium has been fully established and that there is unlikely to be a definitive resolution of this problem in the particular case of PE–surfactant systems.

The charge spacing in the structurally different PEI–surfactant systems is fixed along the chain direction, but there is scope for variation by branching. A proportion of the charges can then be embedded in the polymer structure and are not directly accessible to the surfactant. The charging of the PEI chain can also be modified by pH and by the addition of hydrophilic EO groups and even PO groups. Measurements of surface excess from NR show that a 25k linear PEI interacts strongly with SDS more or less independently of pH from 3 to 10 but does not form anything other than a monolayer. This is consistent with two trends observed for the linear OEI. Starting at the lowest OEI, multilayer formation occurs at pH 3, but as the chain length increases, it occurs only at higher pH. However, multilayer formation also declines when the molecular weight of the OEI reaches 2000, and in the polymer of 25k, it ceases altogether. For two branched PEIs (2k and 25k), the trend suggested by the oligomers is not maintained.⁵⁷ Increasing the size of the branched OEI showed a trend of multilayer formation becoming more prevalent at pH 3 and declining at pH 10, whereas the two polymers form multilayers more strongly at pH 10 and 7 but not at all at pH 3. The failure of the trend to continue probably just reflects the importance of the extent of branching, which cannot be expected to be fully developed by b-EI₁₀ in comparison to a PEI of 40 units, which corresponds to MW = 2000. The ST behavior of the two polymers is consistent with the adsorption, and it is also worth noting that the ST is much lower for PEI–SDS complexes than for the other class of PE–surfactant mixtures.

Multilayer formation of 2k and 25k branched PEI is mainly of the S_2 structure and at higher 2k concentrations of the S_M structure, with only weak S_m for the 25k PEI. The difference with PSS, DNA, PAA, and PVP complexes is that the S_M structures are now not transient but seem to be part of the sequence of surface structures. Again, it is striking that the surface excess of the monolayer formed on the 25k linear PEI is significantly higher than the normal SDS layer, just as with the larger linear OEI. It was postulated above that this was too stable for there to be any need for extra bilayers. Addition of electrolyte further enhances the adsorption, especially for the 2k branched PEI–SDS system, which now shows an extensive range of S_M adsorption.⁵⁸ The addition of an average of one EO per EI to the branched 2k PEI does not disrupt the strong interaction with SDS, and the surface structure is again dominated by the S_m structure, but the addition of three EOs weakens the interaction to that expected for a neutral polymer.⁵⁹

The measurements of surfactant excess by NR show clearly that the fixed in-chain charge separation of linear OEI and PEI favors a highly close-packed SDS layer. This suggests that the lowering of surface energy brought about by the simple S_1 layer cannot be significantly improved by the addition of further bilayers. The intermolecular separation for small OEI will relax the spacing in the S_1 layer, and this allows some formation of multilayered structures. Although the interaction should be weakened by increasing the pH to 10, this is offset by the fixed

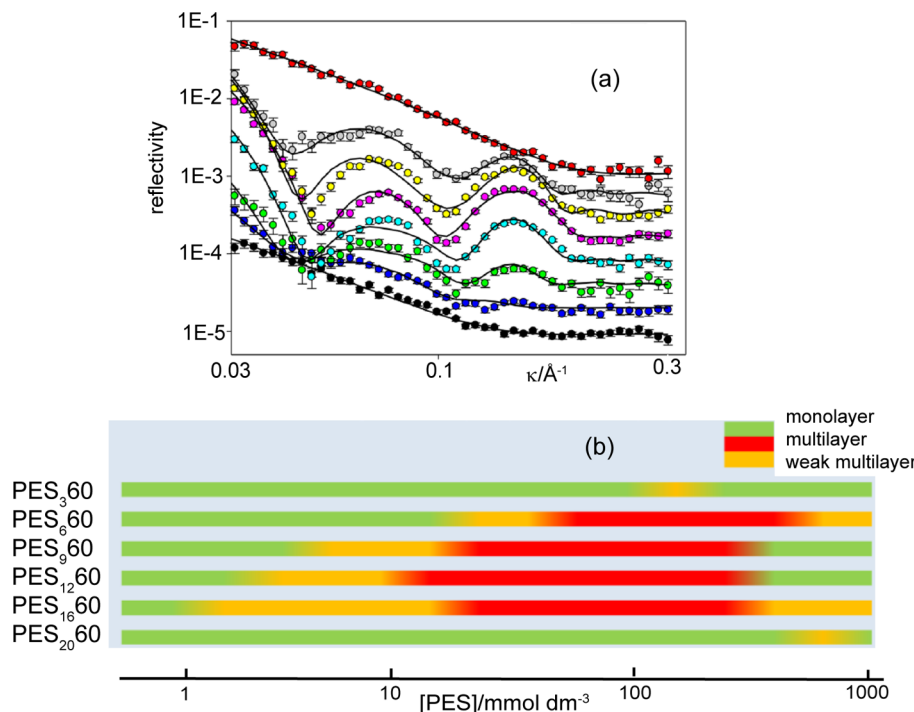


Figure 10. (a) PES₁₂60/0.025 mg/mL hydrophobin in nrw, for PES₁₂60 concentrations between 3.9 and 500 μM . The profiles have been displaced for clarity. (b) Phase diagram for PES_m60 for $m = 3$ to 20.^{66,67}

separation which continues to hold the surfactants at a distance where the coherent hydrophobic interaction is stronger than in a free SDS layer. The linear in-chain charge structure also gives little scope for the formation of cross-links. The other types of polyelectrolytes are also linear, but their charges are generally highly suited to cross-linking between layers, although the energy required to rotate charges into line will be highly variable. The natural situation would then seem to be the formation of an incomplete monolayer of surfactant (relative to pure surfactant) which then gains further surface energy by cross-linking to a bilayer. However, depending on other factors such as the hydrophobicity of the PE, its rigidity, and the size of the surfactant headgroup, the initial monolayer may be close packed enough that the S₁ structure is more stable than S₂. Neither of these effects should be sensitive to the molecular weight. For branched PEI, the effective charge separation for direct interaction with the surfactant headgroup is significantly larger than in linear PEI, and hence an S₁ layer does not realize the full lowering of the surface free energy. In addition, the more rigid structure of the branched chain creates opportunities for cross-linking and further cross-linking. Thus, the S₂ structure forms readily and can continue to S_M. There are now two effects of molecular weight. For a small OEI, the branching can only be minimal and sufficient branching to reduce the density of charge available to the surfactant requires the molecular weight to increase to a threshold which has not yet quite been reached at b-El₁₀. At higher molecular weight, an increase in molecular weight leads to a slow thickening of the PEI which increasingly starts to block the growth of the layer beyond S₁. This evidently occurs somewhere between 2k and 25k because the 2k branched PEI exhibits the strongest layer formation. The interaction of SDS with PEI at pH 10 shows clearly that the combination of a weaker charge interaction with the right surfactant spacing can still generate a strong interaction. This opens the possibility of complexes being

formed between PEI and cationic surfactants. This has been observed but under nonequilibrium conditions,⁶⁰ and we consider it further below.

Hydrophobin–Surfactant Mixtures. Hydrophobins are small globular proteins that are important in the physiology of fungi. The structure of hydrophobin II (HFB II), with which we are concerned here, has been determined at atomic resolution.⁶¹ It is held in a robust conformation by four disulfide bridges, and it has a large well-defined patch of hydrophobicity on one face that makes it extremely surface-active and its A–W surface properties have been extensively studied.^{62–64} Partially because of its fungal origin there is strong interest in applying it to aspects of food technology such as foam stabilization,⁶⁵ and because of its high cost, it needs to be mixed with cheaper materials with minimal loss of functionality. Polyethoxylated sorbates (PES, also called Tweens) are ethoxylated fatty acid sorbitan esters licensed for use in foods and widely used. They consist of an alkanoic acid esterified with sorbitan onto which ethylene oxide is then polymerized to give an average of 20 EO per molecule, divided into 3 or 4 short chains. They are conventionally named according to the alkyl chain, where PES20 designates a C₁₄ chain, PES40 = C₁₆, PES60 = C₁₈, and PES80 = oleic. They are mild surfactants for proteins because of their extensive ethoxylation, but like hydrophobin, they are extremely surface-active in that they have very low CMCs, around 2×10^{-5} M.

It is difficult to determine the separate concentrations of HFBII and the PES at the A–W interface because their scattering-length densities are not very different. To discriminate between them and to contrast any adsorbed layer with the solution, it is necessary to deuterate or partially deuterate one of the components. The ethoxy groups on the PES are not only fairly easy to replace but the total number can be altered. Although the standard PESs have 20 EO, which we designate here as PES₂₀60, and apparently show no unusual surface

behavior, just as found with SDS and $C_{12}E_6$,^{63,64} some of the PESs with less than 20 EO s show strong interference fringes corresponding to the S_3 structure.^{66,67} Figure 10(a) shows the variation of the NR profile of aqueous solutions of 0.025 mg mL⁻¹ HFBII with varying concentrations of partially deuterated PES₁₂60 from 3.9 to 500 μ M in NRW. The reflectivity profiles at low and high concentrations correspond to simple monolayers, but in between, the double-fringe signature of the S_3 structure is very pronounced. The appearance of an S_3 structure in the middle of the concentration range is replicated for PES_m60 for $3 < m < 20$, as shown in Figure 10(b). At a fixed concentration of PES_m60 of 125 μ M, in the middle of the range in the figure, the variation of the HFB II concentration similarly has an optimum range for the appearance of the S_3 structure at around 0.025 mg mL⁻¹. There is also a strong dependence on the alkyl chain length with the concentration range decreasing slightly from the PES80 (oleic acid based) to PES60(stearic acid) and then rapidly until the range of stability for PES20 is quite short.

The structure of the layer is not easy to determine unambiguously except that the double fringe indicates that overall the deuterated part of the layer follows the S_3 structural pattern, i.e., a monolayer of PES followed by two bilayers. Additional information is that the results already described show that both the size of the hydrophilic region and the hydrophobicity of the alkyl chain of the PES are important, i.e., the HFB II and PES must be in close contact. Experiments with the corresponding protonated PES and with D₂O replacing NRW (Figure 11(b)) and using packing arguments based on the known structures of the components lead to the structure shown in Figure 11(a). Apart from the PES molecules in the top hydrophobin layer, the overall PES and HFB II structures follow the S_3 pattern.

HFBII is negatively charged at the pH of the experiments above, but although anionic and nonionic surfactants interact attractively, the structure of the layer does not suggest a charge interaction. However, what it does show is that there is considerable potential for fine-tuning surfactant structure beyond the simple levels that are presently used to optimize their ability to separate membrane surfactants. Finally, we note that the HFBII-PES system is a very powerful hydrophobing agent. This is in sharp contrast to the other systems so far studied in the Adsorption of Concentrated Lamellar Phases section, many of which are equally powerful wetting agents to the extent of being able to wet Teflon.

■ OTHER SYSTEMS

There has been much discussion about whether several of the surface structures described so far are truly equilibrium states or just steady states, especially the PE-surfactant mixtures. This is a question that will always be hard to answer as discussed in the Introduction. However, there are also systems where non-equilibrium conditions are deliberately applied to an A-W interface, which leads to multilayered structures. We consider two examples. The first uses evaporation to create a water gradient across the A-W interface as a means of generating composite polymer-surfactant films, and the second couples a chemical reaction (hydrolysis of tetraethoxysilane (TEOS)) to the self-assembly of a surfactant at the A-W interface to generate ordered structures, which are precursors of the type of mesoporous materials that have become such versatile catalysts.

Edler et al. have followed the development of multilayered thick films of PEI and various cationic surfactants at an open

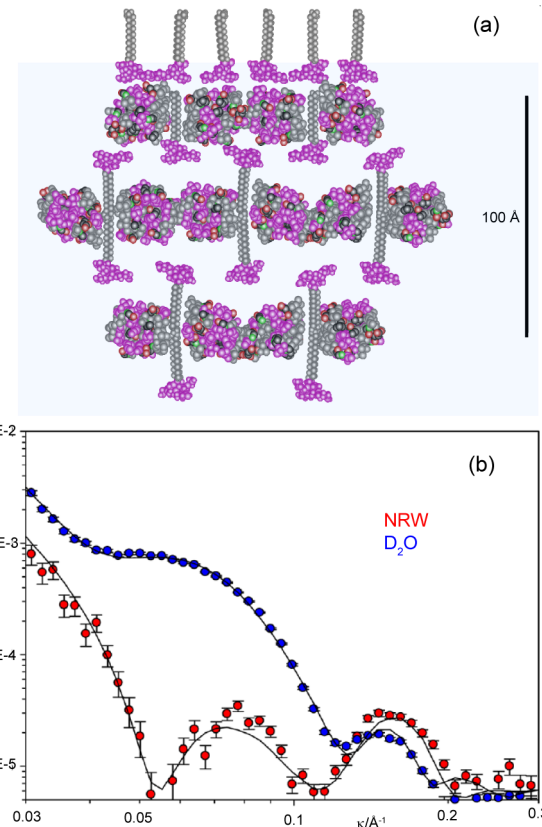


Figure 11. (a) Schematic representation of the hydrophobin/polyethoxylated sorbate surfactant surface structure. (b) NR data for 50 M PES₈60/0.05 mg mL⁻¹ HFB II in NRW and in D₂O. The solid lines are model calculations for the structure shown in (a). The interference fringe at $Q \approx 0.08 \text{ \AA}^{-1}$ arises from the total film thickness, and the fringe at $Q \approx 0.15 \text{ \AA}^{-1}$ results from the bilayer structure and is a broadened Bragg peak.^{66,67}

surface, i.e., in a state of evaporation.^{60,68} The PEI is typically of high molecular weight, 750k, and is used at a concentration on the order of 1 wt % with the cationic surfactant at a concentration usually a little below its CMC. Although small-angle scattering indicates no aggregates in the bulk solution, the composite micrometer-thick film that develops at the surface has a layered structure with a d spacing of about 50 Å, and GIXD has established that the surfactant is in the form of rodlike micelles arranged in layers of 2D hexagonal structure. Although this has superficial similarity to some of the PE-surfactant structures discussed above, it is almost certainly not related. The PEI is at a much higher concentration (about 50-fold) than in the experiments that produce the S_2 and S_3 structures described above, close to concentrations that lower the CMC of surfactant progressively as the concentration increases by amounts typical of weak polymer-surfactant interactions. As evaporation proceeds, the PEI concentration in the surface region can easily increase to a concentration that induces the micellization of the surfactant. As has been modeled by the authors, the film is then replicating part of the phase diagram of a more concentrated system, and its internal structure can be explained in these terms.^{22,60} In contrast, the surface structures (S_2 and so forth) in this article are related to lamellar phases that exist in different parts of the phase diagram, but they do not replicate them. Indeed, such experimental evidence that exists (see AOT and DDAB earlier)

shows clearly that the equilibration of water at the A–W interface is complete under the normal conditions of the NR experiment.

Brown et al. have used NR and XRR to follow the evolution of the A–W interface of a solution of C₁₆TAB and C₁₆TABCi mixed with acidified TEOS, which slowly hydrolyzes in aqueous solution to form silicate species.⁶⁹ Although the surfactant concentration is high at 2 wt % ($70 \times \text{CMC}$), the initial A–W interface has only an adsorbed monolayer of surfactant. Over a period that varies with the conditions, particularly temperature, the reflectivity changes until it quite sharply acquires Bragg peaks, corresponding to long-range periodicity. The authors define the last stage as crystallization and the first stage as the induction period. From the development of the structure that they deduce from a combination of XRR and NR, it is clear that their induction period corresponds to our stages S₁–S_m with m up to about 5, and their crystallization corresponds to the formation of S_M. The spacing in S_M of 45 Å is independent of the counterion, i.e., Cl[−] or Br[−], and gravimetric analysis of the film shows that it contains a large amount of Si. When TEOS hydrolyzes, it initially produces oligomeric silicate species with multiple negative charges, and comparison with the behavior discussed earlier suggests that these species bind to the surfactant cations in ways similar to other oligomers to promote the formation of S₂ structures. However, unlike the systems discussed earlier the concentration and/or length of these oligomers continues to increase by hydrolysis. This leads to kinetic control of the growth in contrast to the fixed concentration or fixed oligomer length experiments of the oligomeric or polymeric systems discussed earlier. By repetitive addition of identical bilayers, kinetic control must lead to a multilayer structure, whereas many of the systems described earlier stop at S₂, S₃, or S_m. As well as this different pattern of buildup of the layers, there will continue to be chemical (e.g., release of ethanol from TEOS) and physical changes in the starting layers. Thus, GIXD shows that the silica develops a well-defined hexagonal structure in the crystallized film,⁷⁰ and the question then arises as to whether the surfactant initially assembles as layers or hexagonally arranged rods. Ruggles et al. have further explored this question using mainly GIXD with a short time resolution, a range of surfactant chain lengths, and added electrolyte concentration and have found a range of different in-plane structures depending on the original phase diagram of the surfactant.⁷¹

A final example, which in action is also a nonequilibrium system but is predominantly studied under equilibrium conditions, is lung surfactant. The large majority of the work on lung surfactant focuses on its behavior as a monolayer, but attention has been increasingly directed toward the issue of the reservoirs of surface-active material which must reside close to or be attached to the A–W surface and which interact with the monolayer.⁷³ However, there seems to be little consideration of the system as an integral single surface multilayered structure, and we will restrict ourselves to the discussion of only that issue. A recent review by Casals and Canadas⁷⁴ comes close to the idea of treating the system as a single-phase multilayer structure of the kind shown in Figure 1. Thus, Casals and Canadas show several structures drawn as S₃ but with bilayers occasionally making vertical interconnections. These are exactly the kind of structures proposed by Exerowa¹² as creating the connections that make the ST dependent on the presence of bilayers below the surface and therefore creating an integral 3D surface structure. In the discussion so far we have suggested

other mechanisms that can also generate integral surface structures, and it would be surprising if one of the functions of the complex protein and lipid composition of lung surfactant was not to create and maintain a surface phase of phospholipids like one of these structures. The experimental difficulties in observing such structures are considerable, partly for the reasons outlined in the Introduction and partly because of the complexity of the composition and the difficulty of creating samples that are fully representative of the *in vivo* material. The latter can be solved to a limited extent by using one of the several animal extracts that have been successfully used to treat respiratory distress syndrome for many years, but the former problem remains. Thus, the main techniques so far used have been electron microscopy and atomic force microscopy, but these are highly invasive for a study of the A–W interface. NR has been used on one occasion, following the procedures described earlier, to examine pharmacy-grade exogenous lung surfactant solutions of bovine and porcine origin.⁷² One of the results is shown in Figure 12, which has a close general

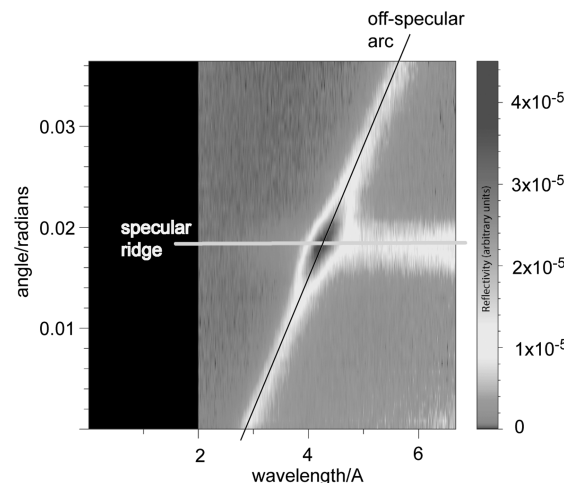


Figure 12. Off-specular neutron scattering from the surface of exogenous porcine surfactant (0.15 wt %) in D₂O with Ringer and added SP-A. The horizontal axis differs from that in Figure 3 in that wavelength is used instead of Q_z , so the pattern is effectively reversed.⁷²

resemblance to Figure 3(c) for an L_α(c) phase but with a larger spacing of about 80 Å. The scattering was investigated in several physiological electrolyte solutions at a surfactant concentration of 0.15 wt %, which is still well below that used in therapeutic application. In all cases, a lamellar stack of the kind that gives rise to the pattern in Figure 12, i.e., an S_M surface structure, was present, and the spacings were mostly in the same range as found for a bulk sample of a swollen bovine extract.⁷⁵ That a successful therapeutic formulation should form a multilayer structure suggests that the actual system may function in a similar fashion.

CONCLUSIONS

We have demonstrated that self-assembly at an A–W interface can be much more complicated than the simple monolayer that is normally assumed and that this is often related to lamellar surfactant phases which are held together by attractive forces, i.e., non-space-filling lamellar phases. The structures formed at the interface form a new class of self-assembled structures, which may have interesting applications through their strong

wetting or nonwetting properties. They could also contribute useful experimental information with respect to the attractive forces between bilayers and to a better understanding of the initial dynamics of formation of a variety of complex structures.

■ ASSOCIATED CONTENT

Supporting Information

Additional references concerning wetting and prewetting, the theory of off-specular scattering, and the study of the effects of trivalent cations on anionic surfactants. This material is available free of charge via the Internet at <http://pubs.acs.org>.

■ AUTHOR INFORMATION

Corresponding Author

*E-mail: robert.thomas@chem.ox.ac.uk.

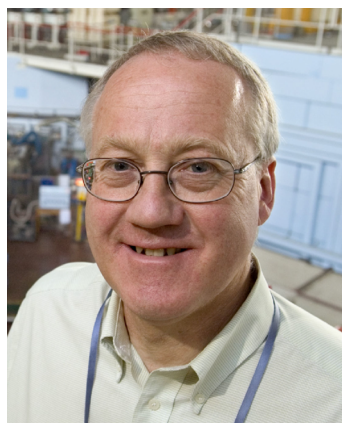
Notes

The authors declare no competing financial interest.

Biographies



Bob Thomas is emeritus in the chemistry department at Oxford, where he was a postdoctoral student, lecturer, and then reader for 45 years, of which 40 have been in the field of neutron scattering, especially neutron reflectometry. He has a joint program of research with Jeff Penfold, which is presently focused on using neutron scattering techniques to explore the surface behavior of surfactants, polymer/surfactant systems, surfactant mixtures, and biosurfactants. He is a fellow of the Royal Society.



Jeff Penfold is emeritus at STFCs Rutherford Appleton Laboratory and ISIS neutron facility, where he was a senior fellow, and a visiting professor in the chemistry department at Oxford. His joint research with Bob Thomas and Unilever has a wide program in colloid and interface science. His research, exploiting neutron scattering techniques to study surfactant and mixed surfactant adsorption and

self-assembly, biosurfactants, polymer–surfactant mixtures, functionalized surfaces, and processing, has resulted in some 400 papers.

■ REFERENCES

- (1) Shinoda, K.; Hirai, T. Ionic Surfactants Applicable in the Presence of Multivalent Cations. Physicochemical Properties. *J. Phys. Chem.* **1977**, *81*, 1842–1845.
- (2) Khan, A.; Fontell, K.; Lindman, B. Liquid Crystallinity in Systems of Magnesium and Calcium Surfactants Phase Diagrams and Phase Structures in Binary Aqueous Systems of Magnesium and Calcium Di-2-ethylhexylsulfosuccinate. *J. Colloid Interface Sci.* **1984**, *101*, 193–200.
- (3) Khan, A.; Lindman, B.; Shinoda, K. Some Observations on Phase Diagrams and Structure in Binary and Ternary Systems of Sodium and Calcium Dodecyl (monooxyethylene) Sulfate. *J. Colloid Interface Sci.* **1989**, *128*, 396–406.
- (4) Wennerstrom, H.; Khan, A.; Lindman, B. Ionic Surfactants with Divalent Counterions. *Adv. Colloid Interface Sci.* **1991**, *34*, 433–449.
- (5) Guldbrand, L.; Jonsson, B.; Wennerstrom, H.; L, P. Electrical double layer forces. A Monte Carlo study. *J. Chem. Phys.* **1984**, *80*, 2221–2228.
- (6) Jho, Y. S.; Kim, M. W.; Safran, S. A.; Pincus, P. A. Lamellar phase coexistence induced by electrostatic interactions. *Eur. Phys. J. E* **2010**, *31*, 207–214.
- (7) Zapf, A.; Beck, R.; Platz, G.; Hoffmann, H. Calcium surfactants: a review. *Adv. Colloid Interface Sci.* **2003**, *100* -102, 349–380.
- (8) Dubois, M.; Zemb, T. Phase Behavior and Scattering of Double-Chain Surfactants in Diluted Aqueous Solutions. *Langmuir* **1991**, *7*, 1352–1360.
- (9) Dubois, M.; Zemb, T.; Belloni, L. Osmotic pressure and salt exclusion in electrostatically swollen lamellar phases. *J. Chem. Phys.* **1992**, *96*, 2278–2286.
- (10) Dubois, M.; Zemb, T.; Fuller, N.; Rand, R. P.; Parsegian, V. A. Equation of state of a charged bilayer system: Measure of the entropy of the lamellar-lamellar transition in DDABr. *J. Chem. Phys.* **1998**, *108*, 7855–7869.
- (11) Pashley, R. M.; McCuiggan, P. M.; Ninham, B. W.; Brady, J.; Evans, D. F. Direct Measurements of Surface Forces between Bilayers of Double-Chained Quaternary Ammonium Acetate and Bromide Surfactants. *J. Phys. Chem.* **1986**, *90*, 1637–1642.
- (12) Kashchiev, D.; Exerowa, D. Structure and Surface Energy of the Surfactant Layer on the Alveolar Surface. *Eur. J. Biophys.* **2001**, *30*, 34–41.
- (13) Takumi, H.; Noda, M.; Matsubara, H.; Takiue, T.; Aratono, M. Dynamics of Condensed Monolayer and Multilayer Formation of Hexadecylpyridinium Chloride-Sodium Dodecyl Sulfate Mixed Systems at the Air/Water Interface. *Chem. Lett.* **2012**, *41*, 1218–1220.
- (14) Monteux, C.; Llauro, M.; Baigl, D.; Williams, C. E.; Anthony, O.; Bergeron, V. Interfacial Microgels Formed by Oppositely Charged Polyelectrolytes and Surfactants. 1. Influence of Polyelectrolyte Molecular Weight. *Langmuir* **2004**, *20*, 5358–5366.
- (15) Hamilton, W. A. Conformation, directed self-assembly and engineered modification: some recent near surface structure determinations by grazing incidence small angle X-ray and neutron scattering. *Curr. Opin. Colloid Interface Sci.* **2005**, *9*, 390–395.
- (16) Bergeron, V.; Claesson, P. M. Structural forces reflecting polyelectrolyte organization from bulk solutions and within surface complexes. *Adv. Colloid Interface Sci.* **2002**, *96*, 1–20.
- (17) Li, Z. X.; Lu, J. R.; Thomas, R. K.; Weller, A.; Penfold, J.; Webster, J. R. P.; Sivia, D. S.; Rennie, A. R. Conformal Roughness in the Adsorbed Lamellar Phase of Aerosol-OT at the Air-Water and Liquid-Solid Interfaces. *Langmuir* **2001**, *17*, 5858–5864.
- (18) Li, Z. X.; Lu, J. R.; Thomas, R. K.; Penfold, J. Neutron Specular and Off-specular Reflection from the Surface of Aerosol-OT Solutions above the Critical Micelle Concentration. *Faraday Discuss.* **1996**, *104*, 127–138.
- (19) Fontell, K. The Structure of the Lamellar Liquid Crystalline Phase in Aerosol OT-Water System. *J. Colloid Interface Sci.* **1973**, *44*, 318–329.

- (20) Li, Z. X.; Weller, A.; Thomas, R. K.; Rennie, A. R.; Webster, J. R. P.; Penfold, J.; Heenan, R. K.; Cubitt, R. Adsorption of the Lamellar Phase of Aerosol-OT at the Solid-Liquid and Air-Liquid Interfaces. *J. Phys. Chem. B* **1999**, *103*, 10800–10806.
- (21) Hellsing, M. S.; Rennie, A. R.; Hughes, A. V. Adsorption of Aerosol-OT to Sapphire: Lamellar Structures Studied with Neutrons. *Langmuir* **2011**, *27*, 4669–4678.
- (22) Aberg, C.; Sparre, E.; Edler, K. J.; Wennerstrom, H. Non-equilibrium Phase Transformations at the Air-Liquid Interface. *Langmuir* **2009**, *25*, 12177–12184.
- (23) Salamat, R.; de Vries, G.; Kaler, E. W.; Satija, S.; Sung, L. Undulations in Salt-Free Charged Lamellar Phases Detected by Small Angle Neutron Scattering and Neutron Reflectivity. *Langmuir* **2000**, *16*, 102–107.
- (24) Bindell, J. B.; Wainfan, N. The Non-Specular Scattering of X-rays from Thin Films. *J. Appl. Crystallogr.* **1970**, *3*, 503–516.
- (25) Pynn, R. Diffuse Neutron Scattering Signatures of Rough Films. *Proc. SPIE* **1992**, *1738*, 270–281.
- (26) Langridge, S.; Schmalian, J.; Marrows, C. H.; Dekadjevi, D. T.; Hickey, B. J. A neutron study of magnetic domain correlations in antiferromagnetically coupled multilayers. *J. Appl. Phys.* **2000**, *87*, 5750–5752.
- (27) McGillivray, D. J.; Thomas, R. K.; Rennie, A. R.; Penfold, J.; Sivia, D. S. Ordered Structures of Dicahn Cationic Surfactants at Interfaces. *Langmuir* **2003**, *19*, 7719–7726.
- (28) Haas, S.; Hoffmann, H.; Thunig, C.; Hoinkis, E. Phase and Aggregation Behaviour of Double Chain Cationic Surfactants from the Class of N-alkyl-N-alkyl'-N,N-dimethylammonium Bromide Surfactants. *Colloid Polym. Sci.* **1999**, *277*, 856–867.
- (29) Penfold, J.; Sivia, D. S.; Staples, E.; Tucker, I.; Thomas, R. K. Surface Ordering in Dilute Dihexadecyl Dimethyl Ammonium Bromide Solutions at the Air-Water Interface. *Langmuir* **2004**, *20*, 2265–2269.
- (30) Brady, J. E.; Evans, D. F.; Warr, G. G.; Grieser, F.; Ninham, B. W. Counterion Specificity as the Determinant of Surfactant Aggregation. *J. Phys. Chem.* **1986**, *90*, 1853–1859.
- (31) Tucker, I.; Penfold, J.; Thomas, R. K.; Grillo, I.; Barker, J. G.; Mildner, D. F. R. The Surface and Solution Properties of Dihexadecyl Dimethylammonium Bromide. *Langmuir* **2007**, *24*, 6509–6520.
- (32) Fameau, A.-L.; Douliez, F.; Boue, J.-P.; Ott, F.; Cousin, F. Adsorption of multilamellar tubes with a temperature tunable diameter at the air/water interface. *J. Colloid Interface Sci.* **2011**, *362*, 397–405.
- (33) Xu, H.; Penfold, J.; Thomas, R. K.; Petkov, J. T.; Tucker, I.; Webster, J. P. R. The Formation of Surface Multilayers at the Air-Water Interface from Sodium Polyethylene Glycol Monoalkyl Ether Sulfate/AlCl₃ Solutions: The Role of the Size of the Polyethylene Oxide Group. *Langmuir* **2013**, *29*, 11656–11666.
- (34) Xu, H.; Penfold, J.; Thomas, R. K.; Petkov, J. T.; Tucker, I.; Webster, J. P. R. The Formation of Surface Multilayers at the Air-Water Interface from Sodium Diethyleneglycol Monoalkyl Ether Sulfate/AlCl₃ Solutions: The Role of the Alkyl Chain Length. *Langmuir* **2013**, *29*, 12744–12753.
- (35) Alargova, R.; Danov, K. D.; Krachevsky, P. A.; Broze, G.; Mehrteab, A. Growth of Giant Rodlike Micelles of Ionic Surfactant in the Presence of Al³⁺ Counterions. *Langmuir* **1998**, *14*, 4036–4049.
- (36) Alargova, R.; Petkov, J.; Petsev, D. Micellization and interfacial properties of alkyloxyethylene sulfate surfactants in the presence of multivalent counterions. *J. Colloid Interface Sci.* **2003**, *261*, 1–11.
- (37) Petkov, J. T.; Tucker, I. M.; Penfold, J.; Thomas, R. K.; Petsev, D. N.; Dong, C. C.; Golding, S.; Grillo, I. The Impact of Multivalent Counterions, Al³⁺, on the Surface Adsorption and Self-Assembly of the Anionic Surfactant Alkyloxyethylene Sulfate and Anionic/Nonionic Surfactant Mixtures. *Langmuir* **2010**, *26*, 16699–16709.
- (38) Penfold, J.; Thomas, R. K.; Dong, C. C.; Tucker, I.; Metcalfe, K.; Golding, S.; Grillo, I. Equilibrium Surface Adsorption Behavior in Complex Anionic/Nonionic Surfactant Mixtures. *Langmuir* **2007**, *23*, 10140–10149.
- (39) Xu, H.; Penfold, J.; Thomas, R. K.; Petkov, J. T.; Tucker, I.; Grillo, I.; Terry, A. Impact of AlCl₃ on the Self-Assembly of the Anionic Surfactant Sodium Polyethylene Glycol Monoalkyl Ether Sulfate in Aqueous Solution. *Langmuir* **2013**, *29*, 13359–13366.
- (40) Xu, H.; Penfold, J.; Thomas, R. K.; Petkov, J. T.; Tucker, I.; Webster, J. P. R.; Grillo, I.; Terry, A. Ion Specific Effects in Trivalent Counterion Induced Surface and Solution Self-Assembly of the Anionic Surfactant Sodium Polyethylene Glycol Monododecyl Ether Sulfate. *Langmuir* **2014**, *30*, 4694–4702.
- (41) Bastardo, L. A.; Meszaros, R.; Varga, I.; Gilyani, T.; Claesson, P. M. Deuterium Isotope Effects on the Interaction between Hyperbranched Polyethylene Imine and an Anionic Surfactant. *J. Phys. Chem. B* **2005**, *109*, 16196–16202.
- (42) Penfold, J.; Thomas, R. K.; Zhang, X. L.; Taylor, D. J. F. Nature of Amine-Surfactant Interactions at the Air-Solution Interface. *Langmuir* **2009**, *25*, 3972–3980.
- (43) Halacheva, S. S.; Penfold, J.; Thomas, R. K.; Webster, J. R. P. Solution pH and Oligoamine Molecular Weight Dependence of the Transition from Monolayer to Multilayer Adsorption at the Air-Water Interface from Sodium Dodecyl Sulfate-Oligoamine Mixtures. *Langmuir* **2013**, *29*, 5832–5840.
- (44) Halacheva, S. S.; Penfold, J.; Thomas, R. K.; Webster, J. R. P. Effect of Architecture on the Formation of Surface Multilayer Structures at the Air–Solution Interface from Mixtures of Surfactant with Small Poly(ethyleneimine)s. *Langmuir* **2012**, *28*, 6336–6347.
- (45) Halacheva, S. S.; Penfold, J.; Thomas, R. K.; Webster, J. R. P. Effect of Polymer Molecular Weight and Solution pH on the Surface Properties of Sodium Dodecylsulfate-Poly(Ethyleneimine) Mixtures. *Langmuir* **2012**, *28*, 14909–14916.
- (46) Jiang, L. X.; Huang, J. B.; Bahramian, A.; Li, P. X.; Thomas, R. K.; Penfold, J. Surface Behaviour, Aggregation and Phase Separation of Aqueous Mixtures of Dodecyl Trimethylammonium Bromide and Sodium Oligoarene Sulfonates: the Transition to Polyelectrolyte-surfactant Behaviour. *Langmuir* **2012**, *28*, 327–338.
- (47) Taylor, D. J. F.; Thomas, R. K.; Penfold, J. The adsorption of Oppositely Charged Polyelectrolyte-Surfactant Mixtures: Neutron Reflection from Dodecyl Trimethylammonium Bromide and Sodium Poly(styrene sulfonate) at the Air-water Interface. *Langmuir* **2002**, *18*, 4748–4757.
- (48) Taylor, D. J. F.; Thomas, R. K.; Li, P. X.; Penfold, J. Adsorption of Oppositely Charged Polyelectrolyte-Surfactant Mixtures: Neutron Reflection from Alkyl Trimethylammonium Bromides and Sodium Poly(styrenesulfonate) at the Air-water Interface: The Effect of Surfactant Chain Length. *Langmuir* **2003**, *19*, 3712–3719.
- (49) Zhang, J.; Taylor, D. J. F.; Li, P. X.; Thomas, R. K.; Wang, J. B.; Penfold, J. Adsorption of DNA and Dodecyl Trimethylammonium Bromide Mixtures at the Air/Water Interface: A Neutron Reflectometry Study. *Langmuir* **2008**, *24*, 1863–1872.
- (50) Zhang, J.; Thomas, R. K.; Penfold, J. Interaction of Oppositely Charged Polyelectrolyte-Ionic Surfactant Mixtures: Adsorption of Sodium Poly(acrylic acid)-Dodecyltrimethyl Ammonium Bromide Mixtures at the Air–Water Interface. *Soft Matter* **2005**, *1*, 310–318.
- (51) Taylor, D. J. F.; Thomas, R. K.; Hines, J. D.; Humphreys, K.; Penfold, J. The Adsorption of Oppositely Charged Polyelectrolyte-Surfactant Mixtures at the Air-water Interface: Neutron Reflection from Dodecyl Trimethylammonium Bromide-sodium Poly(styrene sulfonate) and Sodium Dodecyl Sulfate-poly(vinyl pyridinium chloride). *Langmuir* **2002**, *18*, 978–9791.
- (52) Bahramian, A.; Thomas, R. K.; Penfold, J. The Adsorption Behavior of Ionic Surfactants and Their Mixtures with Nonionic Polymers and with Polyelectrolytes of Opposite Charge at the Air-Water Interface. *J. Phys. Chem. B* **2014**, *118*, 2769–2783.
- (53) Meszaros, R.; Thompson, L.; Bos, M.; Varga, I.; Gilanyi, T. Interaction of Sodium Dodecyl Sulfate with Polyethyleneimine: Surfactant-induced Polymer Solution Colloid Dispersion Transition. *Langmuir* **2003**, *19*, 609–615.
- (54) Mezei, A.; Pojjak, K.; Meszaros, R. Nonequilibrium Features of the Association between Poly(vinylamine) and Sodium Dodecyl Sulfate: the Validity of the Colloid Dispersion Concept. *J. Phys. Chem. B* **2008**, *112*, 9693–9699.

- (55) Campbell, R. A.; Arteta, M. Y.; Angus-Smyth, A.; Nylander, T.; Varga, I. Effects of Bulk Colloidal Stability on Adsorption Layers of Poly(diallyldimethylammonium chloride)-Sodium Dodecyl Sulfate at the Air-Water Interface Studied by Neutron Reflectometry. *J. Phys. Chem. B* **2011**, *105*, 15202–15213.
- (56) Naderi, A.; Claesson, P. M.; Bergstrom, M.; Dedinaite, A. Trapped Non-equilibrium States in Aqueous Solutions of Oppositely Charged Polyelectrolytes and Surfactants: Effects of Mixing Protocol and Salt Concentration. *Colloids Surf., A* **2005**, *53*, 83–93.
- (57) Penfold, J.; Tucker, I.; Thomas, R. K.; Zhang, J. Adsorption of Polyelectrolyte/Surfactant Mixtures at the Air-Solution Interface: Poly(ethyleneimine)/Sodium Dodecyl Sulfate. *Langmuir* **2005**, *21*, 10061–10073.
- (58) Penfold, J.; Tucker, I.; Thomas, R. K.; Taylor, D. J. F.; Zhang, J.; Zhang, X. L. The Impact of Electrolyte on the Adsorption of Sodium Dodecyl Sulfate/Polyethyleneimine Complexes at the Air-Solution Interface. *Langmuir* **2007**, *23*, 3690–3698.
- (59) Zhang, X. L.; Taylor, D. J. F.; Thomas, R. K.; Penfold, J. The role of electrolyte and polyelectrolyte on the adsorption of the anionic surfactant, sodium dodecylbenzenesulfonate, at the air-water interface. *J. Colloid Interface Sci.* **2011**, *356*, 656–664.
- (60) Comas-Rojas, H.; Enriquez-Victorero, C.; Roser, S. J.; Edler, K. J.; Perez-Gramatges, A. Self-assembly and phase behaviour of PEI: cationic surfactant aqueous mixtures forming mesostructured films at the air/solution interface. *Soft Matter* **2013**, *9*, 4003–4014.
- (61) Hakanpaa, J.; Paananen, A.; Askolin, S.; Nakari-Setala, T.; Parkkinen, T.; Penttila, M.; Linder, M. B.; Rouvinen, J. Atomic Resolution Structure of the HFBII Hydrophobin, a Self-assembling Amphiphile. *J. Biol. Chem.* **2004**, *279*, 534–539.
- (62) Linder, M. B. Hydrophobins: Proteins that self assemble at interfaces. *Curr. Opin. Colloid Interface Sci.* **2009**, *14*, 356–363.
- (63) Zhang, X. L.; Penfold, J.; Thomas, R. K.; Tucker, I. M.; Petkov, J. T.; Bent, J.; Cox, A.; Campbell, R. A. Adsorption Behavior of Hydrophobin and Hydrophobin-Surfactant Mixtures at the Air-Water Interface. *Langmuir* **2011**, *27*, 11316–11323.
- (64) Penfold, J.; Thomas, R. K.; Shen, H. H. Adsorption and self-assembly of biosurfactants studied by neutron reflectivity and small angle neutron scattering: glycolipids, lipopeptides and proteins. *Soft Matter* **2012**, *8*, 578–591.
- (65) Green, A. J.; Littlejohn, K. A.; Hooley, P.; Cox, P. W. Formation and stability of food foams and aerated emulsions: Hydrophobins as novel functional ingredients. *Curr. Opin. Colloid Interface Sci.* **2013**, *18*, 292–301.
- (66) Tucker, I. M.; Petkov, J. T.; Penfold, J.; Thomas, R. K.; Li, P. X.; Cox, A.; Hedges, N.; Webster, J. R. P. Spontaneous Surface Self-Assembly in Protein-Surfactant Mixtures: Interactions between Hydrophobin and Ethoxylated Polysorbate Surfactants. *J. Phys. Chem. B* **2014**, *118*, 4867–4875.
- (67) Penfold, J.; Thomas, R. K.; Li, P. X.; Petkov, J. T.; Tucker, I. M.; Cox, A.; Hedges, N.; Webster, J. R. P.; Skoda, M. W. A. Impact of the Degree of Ethoxylation of the Ethoxylated Polysorbate Nonionic Surfactant on the Surface Self-Assembly of Hydrophobin-Ethoxylated Polysorbate Surfactant Mixtures. *Langmuir* **2014**, *30*, 9741–9751.
- (68) O'Driscoll, B. M. D.; Milsom, E.; Fernandez-Martin, C.; White, L.; Roser, S. J.; Edler, K. J. Thin Films of Polyethylenimine and Alkyltrimethylammonium Bromides at the Air/Water Interface. *Macromolecules* **2005**, *38*, 8785–8794.
- (69) Brown, A. S.; Holt, S. A.; Reynolds, P. A.; Penfold, J.; White, J. W. Growth of Highly Ordered Thin Silicate Films at the Air-Water Interface. *Langmuir* **1998**, *14*, 5532–5538.
- (70) Holt, S. A.; Foran, G. J.; White, J. W. Observation of Hexagonal Crystalline Diffraction from Growing Silicate Films. *Langmuir* **1999**, *15*, 2540–2542.
- (71) Ruggles, J. L.; Holt, S. A.; Reynolds, P. A.; White, J. W. Synthesis of Silica Films at the Air/Water Interface: Effect of Template Chain Length and Ionic Strength. *Langmuir* **2000**, *16*, 4613–4619.
- (72) Follows, D.; Tiberg, F.; Thomas, R. K.; Larsson, M. Multilayers at the surface of solutions of exogenous lung surfactant: direct observations by neutron reflection. *Biochim. Biophys. Acta, Biomembr.* **2007**, *1768*, 228–235.
- (73) Mao, G. R.; Desai, J.; Flach, C. R.; Mendelsohn, R. Structural Characterization of the Monolayer-Multilayer Transition in a Pulmonary Surfactant Model: IR Studies of Films Transferred at Continuously Varying Surface Pressures. *Langmuir* **2008**, *24*, 2025–2034.
- (74) Casals, C.; Canada, O. Role of lipid ordered/disordered phase coexistence in pulmonary surfactant function. *Biochim. Biophys. Acta* **2012**, *1818*, 2550–2562.
- (75) Gulik, A.; Tchoreloff, P.; Proust, J. A conformation transition of lung surfactant lipids probably involved in respiration. *Biophys. J.* **1994**, *67*, 1107–1112.